

**3-D SEISMIC ATTRIBUTES ANALYSIS AND RESERVE ESTIMATION
OF “GURAMALA FIELD”, COASTAL SWAMP DEPOBELT, NIGER
DELTA.**

BY

**OSAKI, LAWSON JACK (B.Sc. Geology Uniport)
PGS/M.Sc./20104842578**

**A THESIS SUBMITTED TO THE POST-GRADUATE SCHOOL,
FEDERAL UNIVERSITY OF TECHNOLOGY, OWERRI, NIGERIA**

**IN PARTIAL FULFILLMENT OF THE REQUIREMENTS FOR THE
AWARD OF MASTER OF SCIENCE (M.Sc.) DEGREE IN
GEOPHYSICS.**

NOVEMBER, 2015

CERTIFICATION

I certify that this work "Seismic Attributes Analysis and Reserve Estimation of the Guramala Field in the Coastal Swamp Depobelt of the Niger Delta" was carried out by Osaki, Lawson Jack (20104842578) in partial fulfillment for the award of the degree of M.Sc in Geophysics in the Department of Geology of the Federal University of Technology Owerri.



Dr. A. Opara
(Principal Supervisor)

15/12/2015
Date



Prof. N.N. Onu
(Co-Supervisor)

14/12/2015
Date



Dr. C. Z. Akaolisa
(Head of Department)

18/12/15
Date



Prof. Bede Anusifonwu
(Dean, School of Physical Sciences)

21/12/2015
Date

Engr. Prof. K. B. Oyoh
(Dean, Postgraduate School)

Date



Prof. K.M. Onuoha
(External Examiner)

23-09-2015
Date

DEDICATION

This work is dedicated to the sovereign Lord, for his love and supremacy, and to all that started this programme with us, wished and strived to complete it but could not make it to the end... “You guys are heroes!!”

ACKNOWLEDGEMENT

I sincerely appreciate the management of MONI PULO PETROLEUM LIMITED for providing all the necessary data and the software used to execute the research work, Particularly to the Executive Vice Chairman (EVC); Pastor (Dr) Seinye O. B. LuLu Briggs, for her relentless effort to a huge and resounding industrial experience I achieved with the Geology and Geophysics (G&G) team and exposure to offshore operations.

I am deeply and truly indebted to my wife; Mrs Opuwari Lawson Jack, my children; Sowari Shalom Lawson Jack, Brian Datom Lawson Jack and Lloyd Tamunoeme Lawson Jack for all their patience, support, and encouragement during the programme and the success of this research, also to my mother; Mrs Felicia Lawson Jack for her understanding, love and prayers during the programme.

A profound gratitude to Dr. Alex .I. Opara (supervisor), who spent a lot of his time going through the thesis and making positive corrections. The orderliness of this work is a result of his contribution. I am also grateful to my co supervisor; Dr chikwendu .N. Okereke, Prof. Alex Selemo, Dr Samuel Onyekuru, the late Dr John O. Nwagbara and all the post graduate lecturers of Geology Department for their contribution to this success story.

ABSTRACT

An integrated seismic interpretation using 3-D seismic data, check shot data and a suite of well logs for four wells were analyzed with the Petrel (seismic to simulation software). The objectives were to carry out a detailed formation evaluation, reservoir characterisation and a 3-D assisted structural interpretation of the densely faulted oil field in the coastal depo-belt of the Niger Delta. RMS amplitude, instantaneous frequency map and interval average extraction maps were extracted on the surfaces which revealed the bright spots and Dim spots on them. The attributes were used to establish the diagnostic ability of 3D seismic attribute analysis in enhancing seismic interpretation, and the importance of petrophysical analysis in economic decision in E&P companies as well as researchers of the mid Miocene to Pliocene, Agbada Formation reservoirs in the coastal swamp depobelt of the Niger Delta basin. The method adopted involved a delineation of the various lithologies from the gamma ray log, identification of reservoirs from the resistivity log, well correlation, determination of petrophysical parameters, horizon and fault mapping, time to depth conversion, attribute analysis and reserve estimation. Two reservoirs named Sand_A and Sand_B were mapped. The petrophysical analysis gave porosity values of reservoir Sand_A ranging from 18.1-20.3% and reservoir Sand_B ranging from 13.10-14.9% across the reservoir. The permeability values of reservoir Sand_A ranged from 63-540md while for reservoir Sand_B it ranged from 18-80md. The Sw values for the reservoir ranges from 38-42% in Well 2, 35.39-68.79% in well 7, 32.28-45.57% in well 9 and 68.79-96.06% in well 11. The volume of shale range from 17-82% across the reservoir Sand_B and 49% in reservoir Sand_A. Seven faults labelled F1, F2, F3, F4, F5, F6, and F7 and Four horizons were mapped. Depth structure maps generated showed a massive Northeast-Southwest trending anticlinal structure. The Reserve estimation was calculated using the empirical formula method with the petrophysical parameter, hence well 2 has 9.3 mmbbls, well 7 has 5.7mmbbls, well 9 has 3.5mmbbls and well 11 has 2.3mmbbls. The petrophysical analysis revealed the presence of oil with a volume that is however not favourable for commercial exploitation. These techniques proved to be very reliable and useful in reservoir characterization and formation evaluation.

TABLE OF CONTENT

Declaration	i
Certification	ii
Dedication	iii
Acknowledgement	iv
Abstract	v
Table of Contents	vi
Chapter One	
Introduction	1
1.0 Background of study	1
1.1 Aim and Objectives of the Research	1
1.2 Statement of Problem Definition	
1.3 Justification of the research work	
1.4 Scope of study	4
1.5 Limitation of study	4
1.6 Location of study area	
1.7 The Geology of Niger Delta	5
Chapter Two	
Literature Review:	6
2.1 Review of previous related literature	7
2.2 Theoretical frame work	7
2.2.1 Basic Principle of Seismic Reflection Prospecting	16
2.2.2 Nature of seismic waves	18
2.2.2.1 Types of seismic waves	18
2.2.2.2 Wave characteristics seismic resolution	20
2.2.2.3 Seismic Resolution	21
2.2.3 Seismic data processing	22
2.2.4 Seismic data interpretation	27
2.2.4.1 Picking of reflections	27
2.2.4.2 Picking of faults	27
2.2.4.3 Picking of horizons	27
2.2.4.4 Loop tying	28
2.2.4.5 Timing and posting of horizons	28

2.2.4.6	Time-to-depth conversion curve	28
2.2.4.7	Seismic maps generation	29
2.2.5	Seismic velocity	31
2.2.5.1	Factors affecting seismic velocity	34
2.2.5.2	Relationship between velocity and porosity	34
2.3	Seismic attributes	35
2.3.1	Classification of seismic attributes	35
2.3.2	Post-stack attributes	36
2.3.2.1	Signal envelope or reflection strength	36
2.3.2.2	Envelope derivative	37
2.3.2.3	Second derivative of envelope	37
2.3.2.4	Instantaneous phase	38
2.3.3	Pre-stack attributes	38
2.4	Well logging	38
2.4.1	Open hole analysis	39
2.4.2	Basic welllog classification	39
2.4.2.2	Porosity log	41
2.4.3.3	Resistivity log	43
2.5	Petrophysical analysis	43
2.5.1	Fundamental of petrophysical parameters	44

Chapter Three

3.0	Materials and methods of study	46
3.1	Materials	46
3.1.1	3D seismic section	46
3.1.2	Geophysical well logs	46
3.1.3	Velocity check shot survey data	46
3.2	Methods of study	48
3.2.1	Structural interpretation	48
3.2.2	Seismic attributes	49
3.2.3	Petrophysical analysis	49
3.2.3.2	Volume of shale	50

3.2.3.3	Porosity	50
3.2.3.6	Water saturation	51
3.2.3.6	Resistivity index	52
3.2.3.7	Bulk volume water	53
3.2.3.8	Hydrocarbon pore volume	53
3.2.3.10	Permeability	54
3.2.3.11	v_{sh} total	54
3.2.3.12	Net thickness	54
3.2.3.13	Net to gross ratio	54
3.2.3.14	Effective porosity	54
3.2.3.15	Storage volume	54
3.2.3.16	Volume of oil resources	55
3.2.3.17	Volume of gas resources	55
3.2.3.18	Volume of oil originally in place	55
3.2.3.19	Volume of gas originally in place	56
3.2.3.20	Direct measurement of hydrocarbon in place	56

Chapter Four

Results, Presentation and Interpretation	71
4.1 Reservoir mapping:	71
4.2 Fault interpretation and horizon mapping.	72
4.3 3D seismic time structural maps	72
4.3.1 Time structural map of horizons	72
4.3.2 Seismic depth structural maps	77
4.5 Seismic time surface attributes	82
4.5.1 Extraction map interpretation	82
4.6 Petro physical Interpretation	88
4.7 Reserve Estimate	89
4.8 Discussion	90

Chapter Five

Discussion, Conclusion and Recommendation	90
5.0 Summary	91
5.1 Conclusion	91
5.2 Recommendation	93

List of tables

2.1 Types of well log that are commonly used in Formation evaluation	40
2.2 Porosity range	45
3.1 Geophysical wireline logs of the study area	48
4.1 Showing calculated petrophysical parameters for sand _A Rservoir	87
4.2 Showing calculated petrophysical parameters for sand _B reservoir	88
4.3 Table 4.3; Showing oil originally in place (OOIP) in the various wells	89

List of Figure

1.1	Map of Niger Delta Showing the Study Location	2
2.1	Index Map of the Niger Delta Showing Province Outline Bounding Structural Features and Minimum Petroleum System	7
2.2	Development of Modern Niger Delta since 35Ma	8
2.3	Stratigraphic Column Showing the Three Formations of the Niger Delta	8
2.4	Conventional Structural Styles in the Niger Delta.	10
2.5	Stratigraphic Traps Resulting from Changes in Depositional Environment	12
2.6	Growth Faults Forming Pathways for Hydrocarbon from Akata Formation to Agbada Formation	13
2.7	Burial History Chart for the Northern Portion of the Niger Delta (Akata/Agbada) Petroleum System	15
2.8	Diagram Showing Wave Motion at Time of Explosion	17
2.9	Diagram Showing Waves Detected by Various Geophones Reflected at Different Interfaces	18
2.10	Elastic Deformations and Ground Particle Motions Associated with the Passage of Body Waves (a) P-waves (b) S-waves	19
2.11	Elastic Deformations and Ground Particle Motions Associated with The Passage of Surface Waves (a) Rayleigh wave (b) Love wave	21
3.1	Basemap Showing the Locations of Wells and NW-SE Direction of Correlation.	48
3.2	Time to Depth Conversion Curves and linear function from the check shot of well 2	51
4.1	Well logs from well 2, well 7, well 9, well 11 wells showing the delineated Reservoir (Sand_A and Sand_B) with Gamma ray, Resistivity logs.	58
4.2	The vertical section (inline 57I7) through well 2, showing the fault pattern and horizons (H1, H2, H3 and H4) picked	59
4.3	The event time structure map of horizon H1(top surface of the Sand_A reservoir) at 2750ms	60
4.4	The event time structure map of horizon H2(base of Sand_A reservoir) at	61

2780ms

- | | | |
|------|---|----|
| 4.5 | The event time structure map of horizon H3 (top of Sand_B reservoir) at 2800ms | 62 |
| 4.6 | The event time structure map of horizon H4 (Base of Sand_B reservoir) at 2850ms | 63 |
| 4.7 | Depth structural map of the top of Sand_A Reservoir at 3300m | 65 |
| 4.8 | Depth structural map of the base of Sand_A Reservoir at 3400m | 66 |
| 4.9 | Depth structure map of the top of Sand_B Reservoir at 3450m | 67 |
| 4.10 | Depth structure map of the base of Sand_B Reservoir at 3500m | 68 |
| 4.11 | RMS Amplitude maps of the horizons (a) Horizon(H1) at 2750ms (b) Horizon (H2) at 2780ms (c) Horizon (H3) at 2800ms (d) Horizon (H4) at -2780ms showing high amplitude zones(sky blue) which is possible Hydrocarbon Accumulation(bright spots) areas | 70 |
| 4.12 | Interval average extraction maps of the horizons (a) Horizon(H1) at 2750ms (b) Horizon (H2) at 2780ms (c) Horizon (H3) at 2800ms (d) Horizon (H4) at -2780ms showing high amplitude zones(red and yellow) which is possible Hydrocarbon Accumulation(bright spots) areas. | 72 |
| 4.13 | Instantaneous frequency maps of the horizons (a) Horizon(H1) at 2750ms (b) Horizon (H2) at 2780ms (c) Horizon (H3) at 2800ms (d) Horizon (H4) at -2780ms showing high amplitude zones(yellow and brown) which is possible Hydrocarbon Accumulation(bright spots) areas. | 73 |

CHAPTER ONE: INTRODUCTION

1.0 BACKGROUND OF STUDY

The prolific demand for hydrocarbon products since the 20th century prompted intensified exploration for oil and gas accumulation in reservoir rock, hence the need to use a more technologically and economically viable method in the exploration and exploitation of oil and gas is inevitable owing to the huge sum of money required for a detailed geophysical survey and the subsequent exploitation via drilling of wells. Today Seismic reflection data and well log data have become an integral part of Seismic interpretation especially in lithological and petrophysical prediction of reservoirs, while the Seismic data provides larger coverage but of low resolution, well data provides higher resolution but at a few scattered location. In order to avert any loss or wastage of resources there is need to properly and adequately characterise the reservoir and evaluate the formation so as to accurately ascertain the hydrocarbon potential of the reservoir and also determine its porosity, permeability, water saturation and reserve estimate. In this research work, 3D seismic reflection data were integrated with well logs to identify and characterise the various reservoir units within the “GURUMARA FIELD” using multidisciplinary approach; petrophysical analysis, structural interpretation and 3D seismic attributes analysis.

1.1 AIM AND OBJECTIVES OF THE RESEARCH

This study is aimed at evaluating the formations and characterizing the reservoirs in the study area in terms of their geological structures and hydrocarbon reserve potentials.

In order to achieve the above goal, the specific objectives of this work are to:

- (1) identify and correlate the reservoir units in the study area using gamma ray and resistivity logs;
- (2) delineate oil and gas contact using both neutron and density logs;
- (3) define the reservoir geometry by correlating well to well;
- (4) carry out petrophysical analysis of the reservoir units;
- (5) generate both time and depth structures maps;
- (6) generate various direct hydrocarbon indicator attributes maps and
- (7) Estimate the hydrocarbons in place of economically viable reservoirs.

1.2 STATEMENT OF PROBLEM

The evaluation of hydrocarbon reserves for economic purposes had come with huge uncertainties due to heterogeneity of the subsurface and poor evaluation of target reservoir bodies, structures and stratigraphic development and overall geologic resolution. This has been a major challenge in the oil industry therefore in order to reduce the numerous uncertainties and inadequate mapping of the subsurface rock properties, hence, seismic attribute analysis was intergrated into to the convectional techniques which are seismic interpretation and Petrophysical analysis.

1.3 JUSTIFICATION OF THE RESEARCH WORK

Economic analysis of potential reservoirs necessitates an understanding of the lateral extent, quality, and predictability of the unit of interest. Thus, the integration of seismic attributes, petrophysical analysis with structural interpretation will help in delineating new reservoirs that might be hidden in structural traps. Insights from this study would reduce exploration risks.

1.4 SCOPE OF STUDY

This work is limited and focus on the analysis and interpretation of the structural history of the study area from the available 3D seismic reflection data and a suite of Geophysical wire line logs from four wells and a velocity check shot survey data, also integrated is seismic attribute analysis for an improve Geologic resolution of hydrocarbon prospect zones of the “GURUMARA FIELD” located at the Coastal Swamp Depo belt of the Niger Delta(fig 1.1).

1.5 LIMITATION OF STUDY

Due to the confidentiality clause binding the collected data it made the collection of the exact coordinates of the field impossible rather a close coordinates were released and unavailability of core sample data of the field reduced the accuracy range of the petrophysical parameters.

1.6 LOCATION OF STUDY AREA

The field under consideration, identified as GURAMARA for the purpose of the study is an offshore oil field located in the coastal swamp depobelt of the Niger Delta, southern Nigeria and covers an area of about 42.8 km² of migrated seismic sections (Figure 1.1). It is situated within longitude 05 degrees 41'27"E to 05 degrees 42'05"E and latitude 05 degree51'55"N to 05 degree22' to 05 degrees 52'03"N around the western part of the African continental

margin at the apex of the Gulf of Guinea, which formed the site of a triple junction during continental break up in the creataceous (Doust,1990).

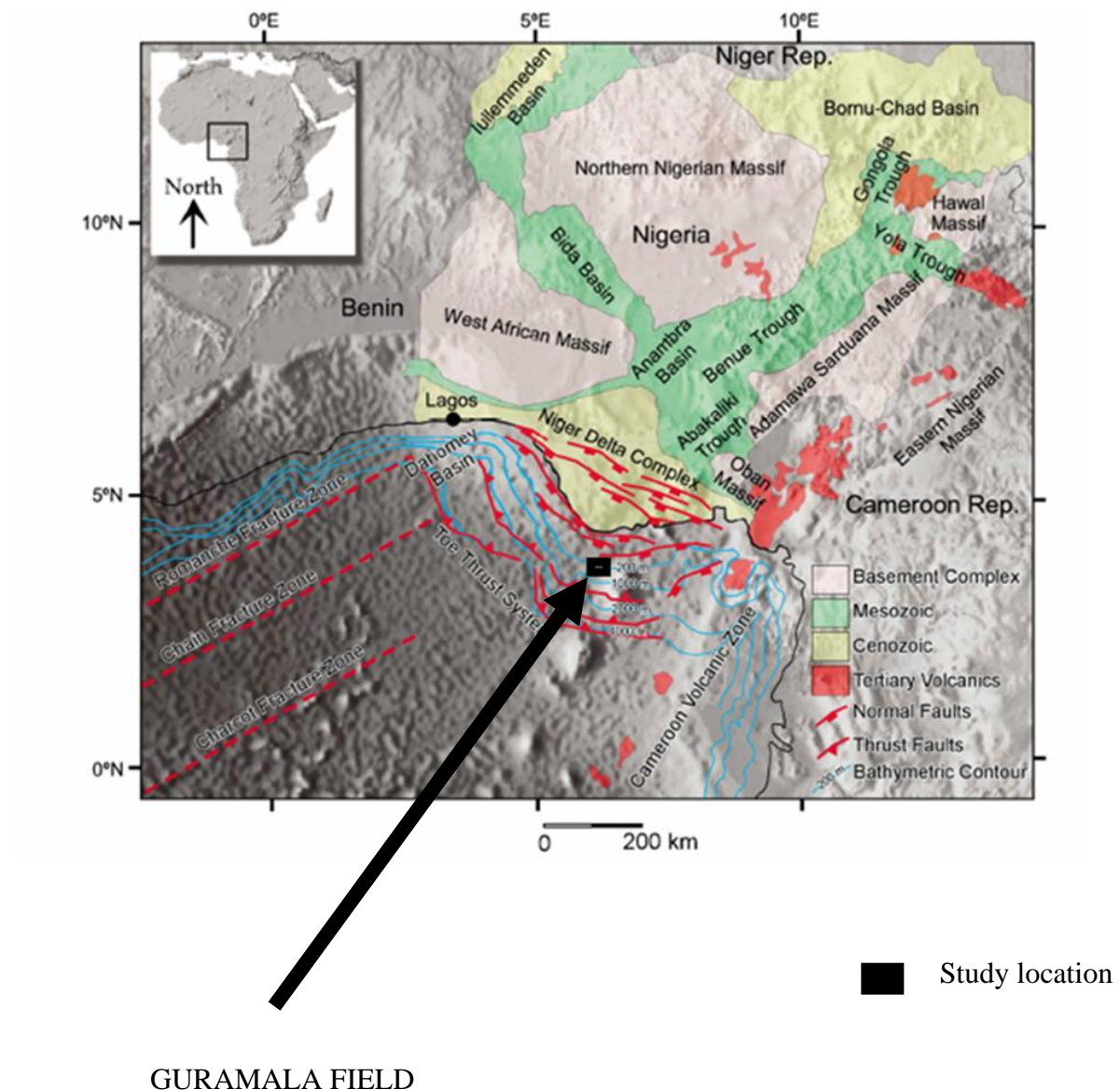


Figure 1.1 Map of Niger Delta Showing the Study Location (After Whiteman, 1982).

1.7 THE GEOLOGY AND GEOMORPHOLOGY OF NIGER DELTA

The Niger Delta is situated in the Gulf of Guinea on the West Coast of Central Africa. It is located in the southern part of Nigeria within latitudes $4^{\circ} 00'N$ to $6^{\circ} 00'N$ and longitudes $3^{\circ} 00'E$ to $9^{\circ} 00'E$ and bounded in the East and West by the Calabar and Benin flanks respectively. In the South it is bounded by the Gulf of Guinea and in the North by the older (Cretaceous) tectonic elements such as the Anambra Basin, Abakaliki uplifts and the Afikpo syncline (Figure 2.1). The Niger Delta is one of the world's largest delta with the subaerial

portion covering about 75,000km² and extending more than 300km from the apex to mouth. The regressive wedge of clastic sediments, which it comprises, is thought to reach a maximum thickness of about 12km. At the mouth of the Benue and Cross river system, it has been built out into the Atlantic with the Niger- Benue river being its main supplier of sediments but with input from the Cross river in the East (Doust and Omatsola, 1990).

Throughout the geological history of the Delta, its structure and stratigraphy have been controlled by the interplay between rates of sediments supply and subsidence. Important influences on sedimentary rates have been eustatic sea level changes and climatic variations in the hinterland. Subsidence has been controlled largely by the initial basement morphology and differential sediment loading on unstable shale (Doust and Omatsola, 1990).

The Delta sequence is extensively affected by syn-sedimentary and post-sedimentary normal faults, which can be traced over considerable distances along strike. The association of source rock, lithology types, structures and thermal histories were some of the conditions favourable for the generation, accumulation and retention of hydrocarbon in the Niger Delta, thus making the Delta prolific in terms of hydrocarbon occurrence.

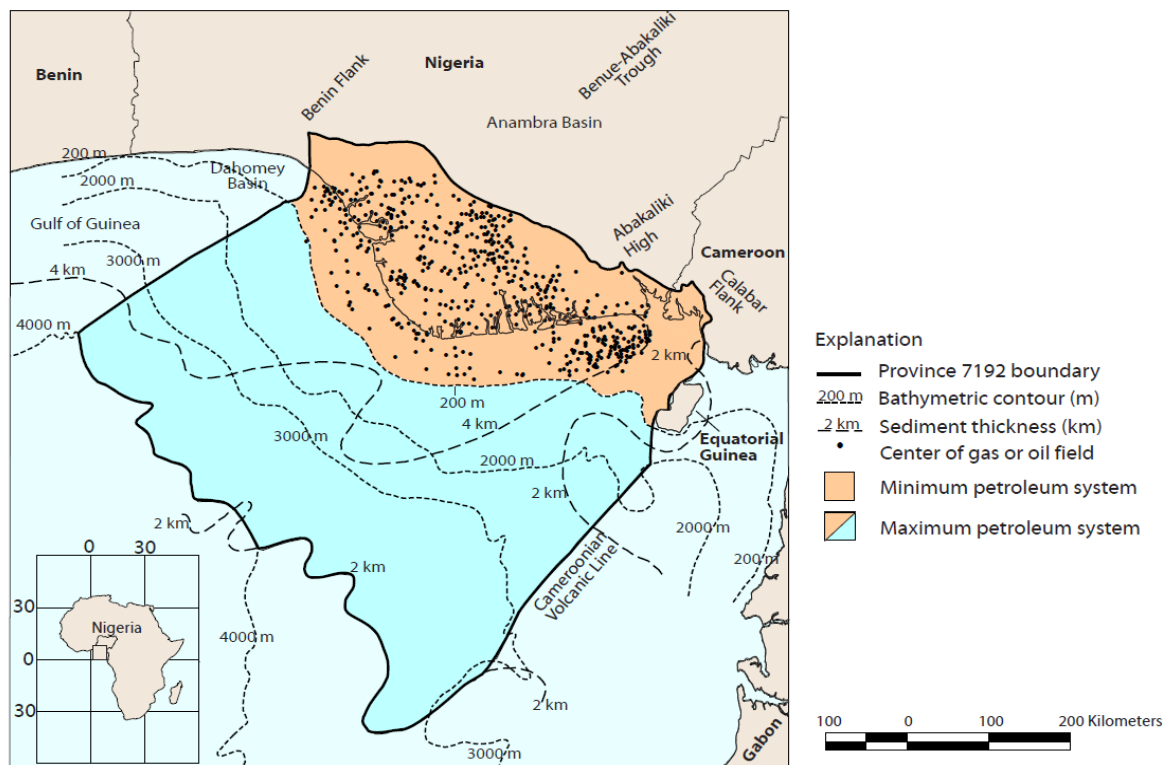


Figure 1.2: Index Map of the Niger Delta Showing Province Outline Bounding Structural Features and Minimum Petroleum System (After Whiteman., 1982).

1.7.1 The Modern Niger Delta

The formation of the modern Niger Delta began in the Eocene era. (Figure 2.2). During the middle and late Eocene, the sedimentary rocks became increasingly sandy, marking the onset of a general regression and of deltaic deposition. The deposition of the more sandy Ameki formation was succeeded by the Ogwashi-Asaba Formation and its equivalent, the Ijebu Formation in the Lagos area, which were of probably Oligocene and Miocene to Recent age. The younger Ogwashi-Asaba and Benin Formation are commonly masked by thick, partly weathered layers of recent Niger delta sediments and by dense vegetation in the south. In the subsurface sedimentary sequences, separate stratigraphic units have been established.

1.7.2 Subsurface Formation of the Tertiary Niger Delta

Three main stratigraphic units underlay the Niger Delta (Figure 2.3). These are the Akata, Agbada and Benin Formations (Short and Stauble, 1967; Frankl and Cordry, 1967; Avbovbo, 1978).

1.7.2.1 The Akata Formation

Akata Formation is the deepest stratigraphic unit, which is chiefly represented by plastic, low density, under compacted and high pressure shallow marine to deep water shales, with only local interbeddings of sands and /or siltstones. It is deposited as the high energy delta advanced into deep water. The depositional environment is typically marine, and the maximum thickness is believed to average 6096 m. It seems to be continuous but diachronous with the outcropping Imo shales. Also, the formation is thermally matured and is considered to be the main source rock of the Niger delta liquid hydrocarbons.

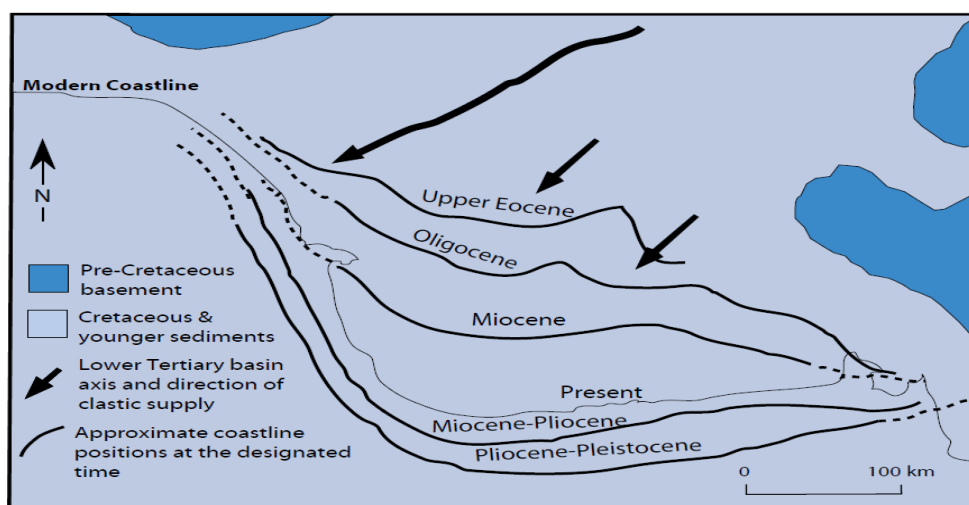


Figure 1.3: Development of Modern Niger Delta since 35Ma (After Whiteman, 1982).

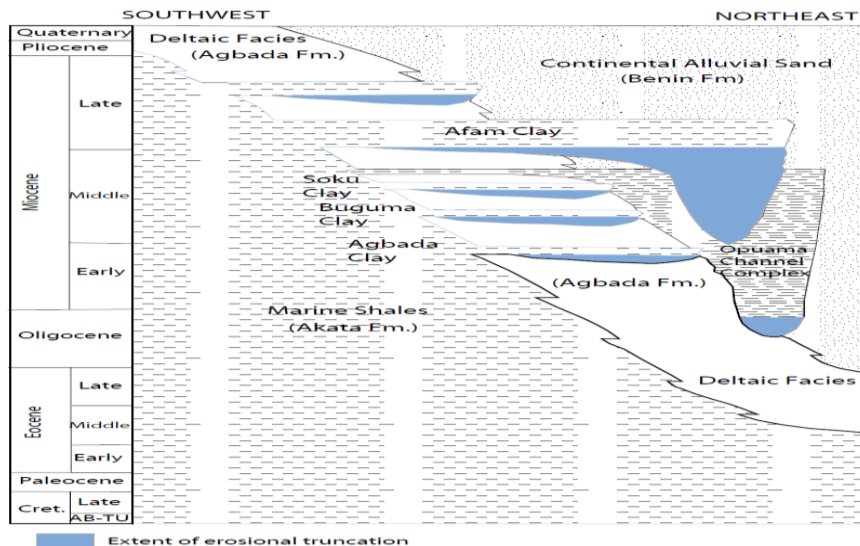


Fig 1.4: Stratigraphic Column Showing the Three Formations of the Niger Delta. (After Shannon and Naylor, 1989; Doust And Omatsola, 1990).

1.7.2.2 The Agbada Formation

This is represented by paralic sequence of interbedded, fluvial, coastal, fluviomarine sands and/or sandstones and intercalated marine shales, underlying the Benin Formation. The upper part is predominantly sandy unit with minor shale intercalation and a lower shaly unit, which is thicker than the upper sandy unit. The depositional environment is therefore defined as “transitional” between the upper continental Benin Formation and the marine underlying Akata Formation. It is Miocene in the North and Pliocene/Pleistocene in the South and has a maximum thickness of possibly 4500 m (Doust and Omatsola, 1990).

This formation is particularly important for oil exploration due to the fact that the greatest part of hydrocarbon occurrences in the Niger Delta has been found in the upper unit of its sandy bodies

1.7.2.3 The Benin Formation

The Benin Formation, mostly of Pliocene age, is the uppermost unit and consists of thick bodies of sands, gravels and plant remains with only local shale and/or sandy shale interbeddings predominantly towards and the maximum thickness of the entire series averages 2100 m. This formation outcrops in Benin, Onitsha, and Owerri area and extends from the west across the entire Niger Delta subsidence of the basement. Identifiable structural

units include point bars, channel fills and natural levees. Very little hydrocarbon accumulation has been associated with this highly porous and generally fresh water bearing formation. The contact between Benin and Agbada Formation is defined at the base by massive sandstones typical of Benin Formation and generally correspond to the base of freshwater bearing strata. The lower part of the formation is probably of Miocene age (Reyment, 1964).

1.7.3 Subsurface Structures in the Niger Delta

The subsurface structures in Niger Delta can be classified into three groups viz; structural traps, stratigraphic traps and combined structural and stratigraphic traps.

1.7.3.1 Structural Traps

Structural traps are structures that arise as a result of folding and faulting (Figure 2.4). Folding however is not a reliable guide in searching for hydrocarbon pool because of a change in shape, size and amplitude in depth, and shift in their lateral position from surface to depth. Folding and faulting that occur below buried unconformities are frequently not indicated at the surface. Pools trapped by normal faulting are almost always on the upper side of the fault because the oil and gas escape up dip around the end of fault. Those that formed in the lower side are rare, if at all found. The majority of the hydrocarbon traps in the Niger Delta are structural. They were formed as a result of syn-sedimentary structural deformation of sediments in the Niger Delta. An important characteristic of structural trap is that they are often capable of providing oil/gas production from a number of horizons.

1.7.3.2 Stratigraphic Traps

This type of traps is created by any variation in the stratigraphy that is essentially independent of structural deformation (due to simple erosion or uncomplicated tilting). Some stratigraphic traps have also been recognized in the Niger Delta (Orife and Avbovbo, 1982). Lithologic, electrical logs and seismic data indicate that stratigraphic traps occur in the Niger Delta in addition to the commonly reported growth fault generated anticlinal traps. The use of the term

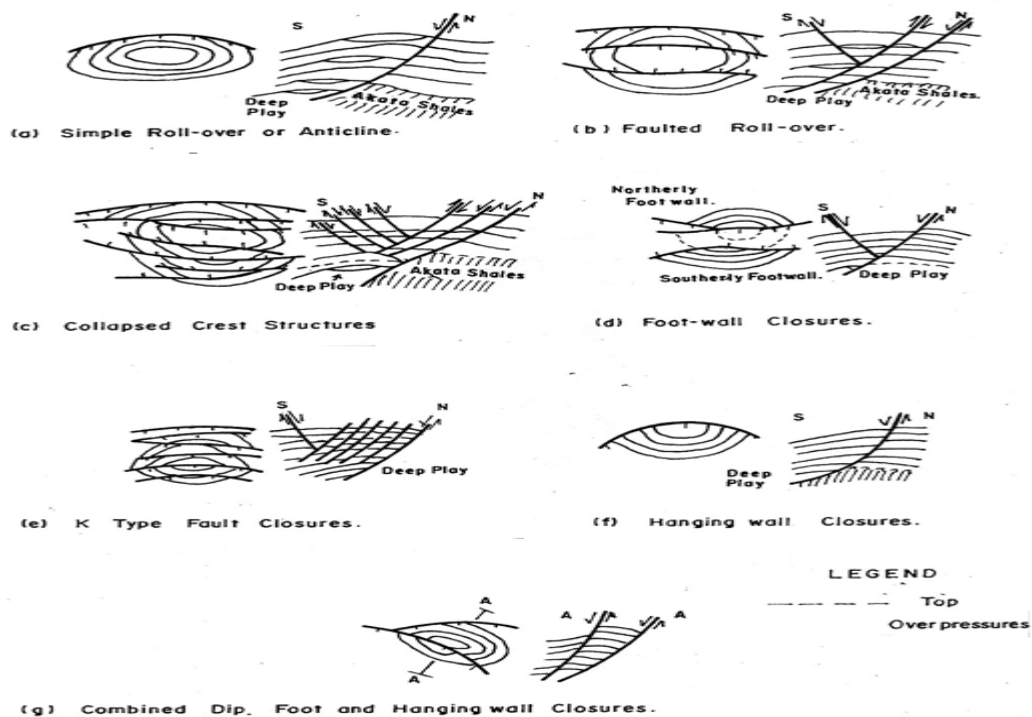


Figure 1.5: Conventional Structural Styles in the Niger Delta. (After SPDC,1992).

“Stratigraphic trap” may be limited to “those traps which are caused by a lateral change in reservoir properties within a given stratum. Stratigraphic traps are sometimes referred to as permeability traps (Figure 2.5). Three types of stratigraphic accumulations are recognized in the Niger Delta. These traps are:

- (1) Crestal accumulations below mature erosion surfaces,
- (2) Canyon- fill accumulations above unconformity surfaces, and
- (3) Facies change traps.

All the various stratigraphic traps observed in the Niger Delta were identified by interpretation of seismic data. Examples of stratigraphic traps that are common in the Niger Delta include the following; Lithologic pinchouts, onlap sand, unconformities wedges, slope channel fills, basin floor fans and turbidities.

1.7.3.3 Combined Structural and Stratigraphic Traps

These are sometime regarded as the third type of traps. These traps are formed by both structural and stratigraphic trap forming mechanisms. They exhibit both structural and stratigraphic features. Instances include a faulted diapiric stratigraphic trap, salt dome- cap rock in reservoir. They are in most cases complex and best trap system.

1.7.4 Hydrocarbon Generation and its Occurrences

Petroleum occurs throughout the Agbada Formation of the Niger Delta. However, several directional trends form an “oil-rich belt” having the largest field and lowest gas: oil ratio (Ejedawe, 1981; Evamy, 1978; Doust and Omatsola, 1990). The belt extends from the Northwest offshore area to the Southeast offshore and along a number of North-South trends in the area of Port-Harcourt. It roughly corresponds to the transition between continental and oceanic crust, and is within the axis of maximum sedimentary thickness. (Tuttle, 1999).

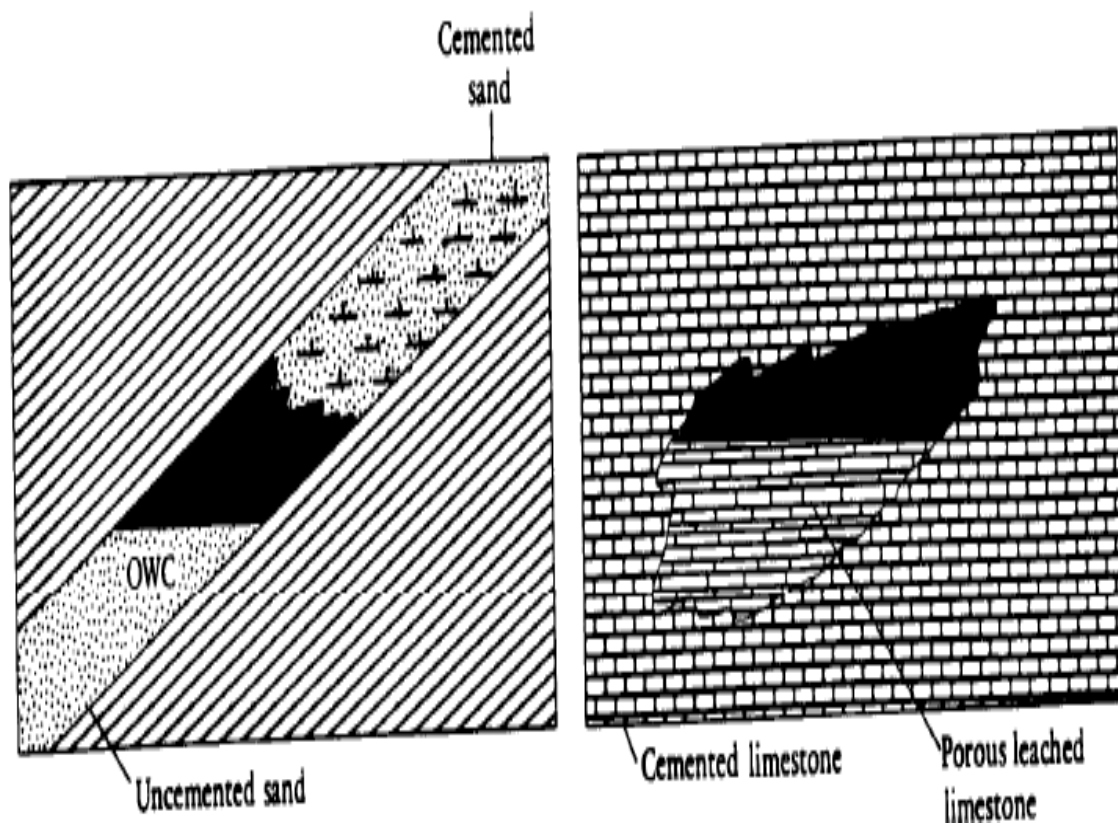


Figure 1.6: Stratigraphic Traps Resulting from Changes in Depositional Environment (After Baker Hughes INTEQ, 1999).

This hydrocarbon distribution was originally attributed to timing of trap formation relative to petroleum migration. Ejedawe (1981) states that the two controlling factors of hydrocarbon flushing of accumulations by gas generated at higher maturity, and/or heterogeneity of source rock type (Doust and Omatsola, 1990). Distribution are on increase in geothermal gradient relative to the minimum gradient in the delta centre and the generally greater age of sediments within the belt relative to those further seaward (Figure 2.6). Together, these factors gave the sediments within the belt the highest “maturity per unit depth”. Weber (1987)

indicates that the oil-rich belt coincides with a concentration of roll over structures across depobelt having short Southern flanks and little paralic sequence to the south. Doust and Omatsola (1990) suggest that the distribution of petroleum is likely related to the heterogeneity of source rock types (greater contribution from paralic sequence in the west) and/or segregation due to remigration. Haack (1997) relates the position of the oil-rich belt to oil-prone marine source rocks deposited adjacent to the delta lobes and suggest that the accumulation of these source rocks was controlled by pre-tertiary structural sub-basins related to basement structures outside the oil- rich belt, the gas: oil ratio (GOR) are high. The GOR within each depobelt increases seaward and along strike away from depositional centres. Causes for the distribution of GOR's are speculative and include remigration induced by tilting during the latter history of deposition within the downpipe portion of the depobelt.

1.7.4.1 Source Rocks

The source rock of the Niger Delta petroleum system has been a controversial topic as expressed in many papers (Evamy , 1978; Ekwezor, 1979; Ekwezor and Daukoru, 1994; Doust (1989). This is as a result of possibilities of variable contributions from the marine interbedded shale in the Agbada Formation and the marine Akata Formation.

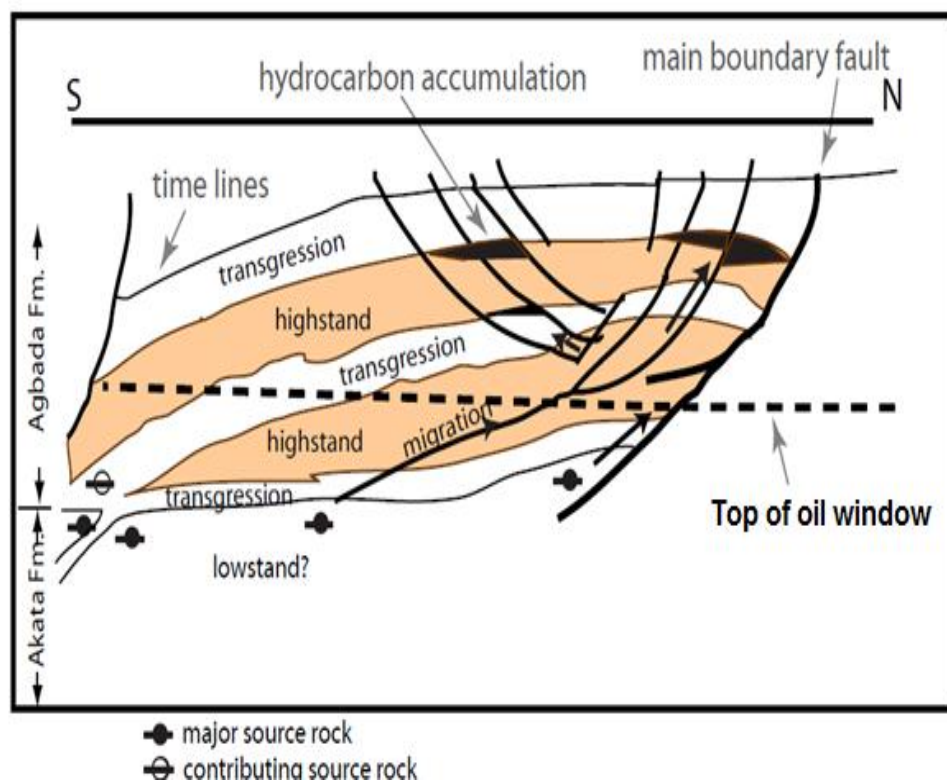


Figure 1.7: Growth Faults Forming Pathways for Hydrocarbon from Akata Formation to Agbada Formation (After Evamy, 1978).

Generally, the main source rock is thought to be shale of the Akata Formation. A delta-wide study of the shale samples indicated that, except for the most eastern part of the delta, the upper part of Akata Formation can be considered as a matured source rocks. The Akata shale has been deposited under anoxic conditions on the continental slope of the delta where the nutrient supply for the planktonic organisms must have been plentiful. Although many shale samples from the lower part of the paralic sequence also have source rock characteristics, a recent study has shown that most of these shale are immature.

1.7.4.2 Reservoir Rocks

Petroleum in the Niger Delta is produced from sandstone and unconsolidated sands predominantly in the Agbada Formation. Characteristics of the reservoirs in the Agbada Formation are controlled by depositional environment and the depth of burial. Known reservoir rocks are Eocene to Pliocene in age, and are often stacked, ranging in thickness from less than 15meters to 10% having greater than 45meters thickness (Evamy,1978).The thicker reservoirs likely represent composite bodies of stacked channels (Doust and Omatsola, 1990).

Based on reservoir geometry and quality, Kulke (1995) described the most important reservoir types as point bars of distributaries channels and coastal barrier bars intermittently cut by sand- filled channels. Doust and Omatsola (1990) described the primary Niger Delta reservoirs as Miocene paralic sandstones with 40% porosity, 2 Darcy's permeability and thickness of 100m. The lateral variation in reservoir thickness is strongly controlled by growth faults; the reservoir thickens towards the fault within the down-thrown block (Weber and Daukoru, 1975). The grain size of the reservoir sandstones is highly variable with fluvial sandstones tending to be coarse than their delta front counterparts; point bars fine upward and barrier bars tend to have the best grain sorting. Much of this sandstone is nearly unconsolidated, some with minor component of argillo-silica cement (Kulke, 1995).In other portion of the delta complex, deep- sea channel sands, low- stand sand bodies and proximal turbidity create potential reservoirs (Beka and Oti, 1995). Burke (1972) described three deep-water fans that have likely been active through much of the delta's history (Figure 2.7).The fans are smaller than those associated with other large deltas, and buried along with the proximal parts of the fans as the position of the successive depobelt move seaward (Burke,1972). The distribution, thickness, shaliness and porosity/permeability characteristics of these fans are poorly understood (Kulke, 1995).

1.7.4.3 Migration

At the level of the Akata Formation, the major growth faults upset a thickness of up to several thousand feet of overpressured shales against paralic sediments in the down thrown block. Applausive migration path may thus be from the overpressured shale into the sand through the sand zones. The sands juxtaposed against overpressured formation are the only down throw block reservoirs which occasionally have hydrocarbon trapped against growth faults, from the conductive fault zones the hydrocarbon appear to the flow into the downthrown blocks. This may be the effect of the specific gravity of the hydrocarbon which tends to bring them into the part of the fault zones, which is adjacent to, the downthrown. A study of the relationship between the level of where hydrocarbons are found and throw of the growth fault indicates that the vertical conductivity of the fault zones of oil probably ceases when the flow drop below 150m, apart from the along-fault migration, other migration route from the Akata Formation shales must be rule out in this respect, the most likely migration path is along regional flanks, i.e. from a seaward facies change updip into the south flank of rollover structures.

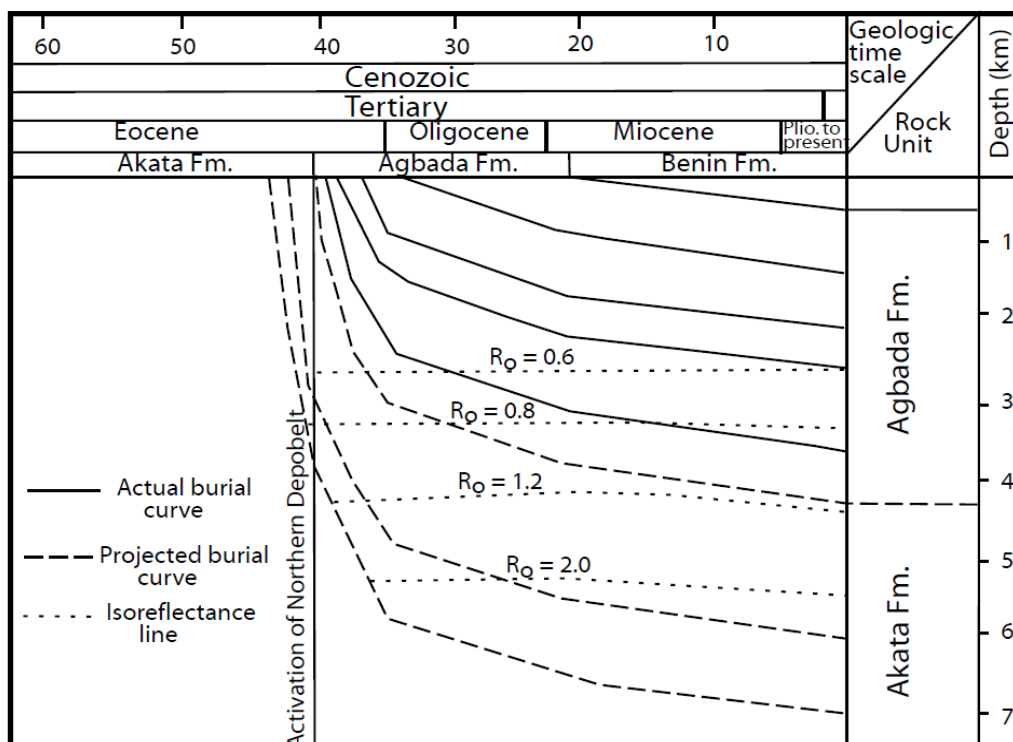


Figure 1.8: Burial History Chart for the Northern Portion of the Nige Delta (Akata/Agbada) Petroleum System (After Ekweozor and Daukoru, 1994).

CHAPTER TWO : LITERATURE REVIEW

2.1 REVIEW PREVIOUS RELATED LITERATURE.

Short and Stauble (1967) and Weber and Daukoru (1975) outlined three major depositional cycles in the coastal sedimentary basins of Nigeria. They first began with an Albian marine incursion and terminated during the Santonian time. The proto-Niger Delta started during the second cycle, while the growth of the Niger Delta continued from Eocene to Recent time. At several stages during the late Quaternary, sedimentation was interrupted by uplift and erosion, whereby several cycles of channels were cut and filled, which resulted to submarine canyons (Evamy,1978).According to Short and Stauble (1967) and Doust and Omatsola (1990), the Niger Delta comprises of a regressive sequence of deltaic and marine clastic, defined by three major lithofacies at the base by marine shale made up of Akata Formation, followed by paralic sequence of Agbada Formation and topmost non-marine alluvial (continental) sands of the Benin Formation.

Weber (1971) reported the cyclic nature of sedimentation of the Tertiary paralic deposits. According to him, a complete cycle of thin, fossiliferous marine sands followed by an offlap sequence, which commences with marine sediments and another transgression may terminate the cycle. Doust and Omatsola (1990) recognized six depobelts in the Niger Delta, which are distinguished primarily by their age. They are Northern delta (late Eocene-Early Miocene), Great Ughelli (Oligocene-Early Miocene), Central swamp I (Early-Middle Miocene), Central Swamp II (middle Miocene), Coastal swamp I and II (Middle Miocene) and offshore mega structures (Late Miocene).

Abe and Olowokere(2013),have interpreted 3D seismic data set from continental slope, offshore Niger Delta integrating structural interpretation with seismic attributes. Their interpretation revealed high amplitude areas in and around area of structural high.

Adeogba (2005) have interpreted a near surface, 3D seismic data set from the Niger Delta continental slope, offshore Nigeria and revealed important stratigraphy and architectural features. Architectural features and sediment deposits interpreted from seismic character and seismic stratigraphy in the absence of borehole data include mass-transport complexes, distributary channels, submarine fans and hemi pelagic drape complex.

Stacher (1995), produced a delta wide framework of cretaceous chronostratigraphically surfaces, and a sequence stratigraphic chart for the Niger Delta, using digitally stored biostratigraphic data, obtained from over 850 wells. Krusi and Idiagbor (1994) linked some types of stratigraphic traps to incised valley fills and low stand fans. They were thus able to improve the identification of stratigraphic plays in eastern Niger Delta. Ozumba (1999), developed a sequence stratigraphic framework of the western Niger Delta, using foraminifera and wire line log data obtained from four wells in the coastal and central swamp depobelts. He concluded that the late Miocene sequences were thicker than the middle Miocene sequences.

Poston (1983) presented the geology and reservoir characteristics at Meren field. They noted evidence for syn-depositional displacement on growth faults across the field. They also suggested combining well-log interpretation and laboratory analyses of sidewall cores to aid in the determination of the spatial variation of porosity and permeability within particular reservoir intervals.

2.2 THEORETICAL FRAMEWORK

Seismic reflection is the most widely employed geophysical technique in oil exploration work. This is because it has the ability to reduce the inherent ambiguities of geophysical method due to its high degree of resolution of the subsurface geology and greater depth of penetration, which make it possible for the study of layered sequences in sedimentary basins and which are the primary targets for oil and gas exploration. Since exploration for hydrocarbons represents one of the major applications of this geophysical method, it is therefore not amazing that seismic exploration gulps about two-third of all the resources allocated to geophysical surveying. Seismic reflection technique involves creating seismic energy sources (shots) at known locations at or below the earth surface and using arrays of devices to record the resultant seismic waves in form of times required by seismic waves to travel from the source to the listening devices called geophones at various distances and locations (Figure 2.8). The primary application of seismic reflection method is in location and mapping of such features as anticline, faults, salt domes, diapirs, reefs and so on, most of which these are associated with the accumulation of oil and gas. Also, it plays an important role in tackling various problems associated with structural geology. Seismic data interpretation is the translation of the physical measurements of the subsurface into geological terms. The acquisition of seismic reflection data starts with the planning and

execution of a seismic reflection survey. This is followed by the processing and finally the interpretation of the processed data. The acquisition of seismic data can be carried out either in frontier area with no substantial well control, or in areas with substantial well control.

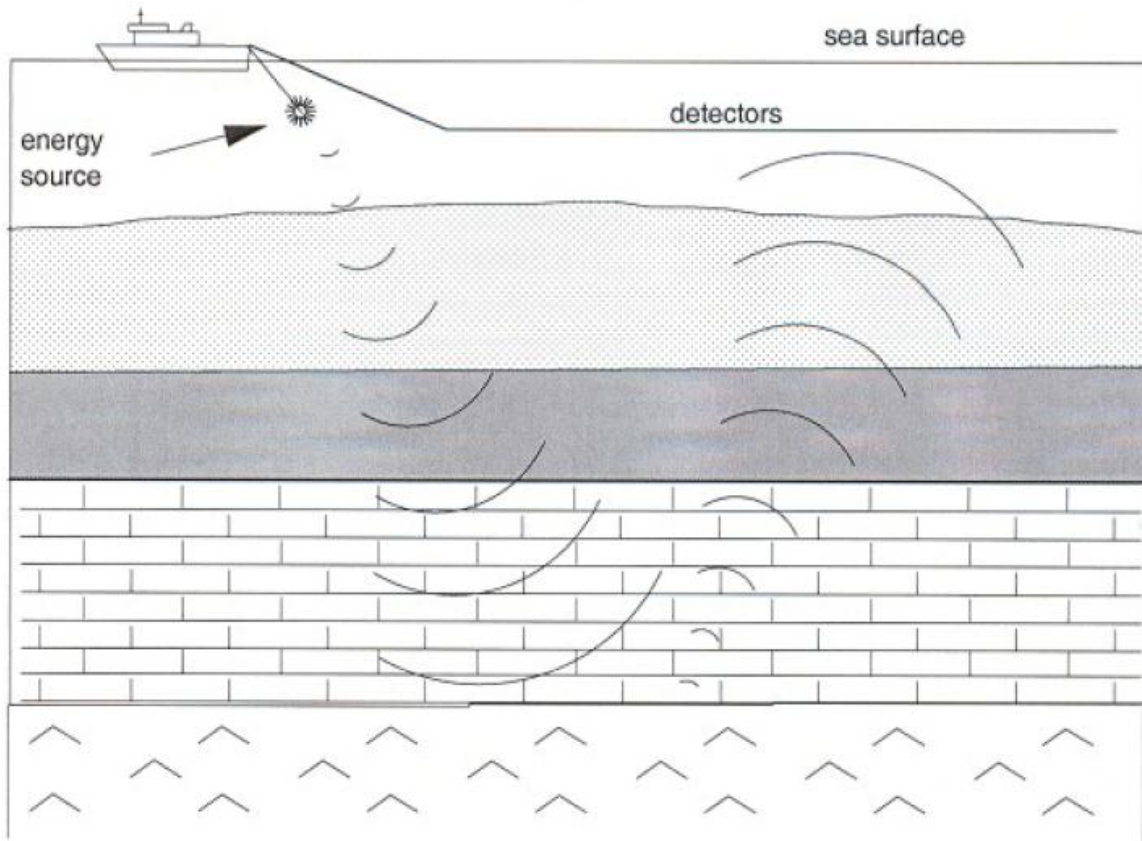


Figure 2.8: Diagram Showing Wave Motion at Time of Explosion (After Dobrin and Savit, 1988).

The data from the frontier areas provide both definition of structure and estimates of depositional environment while in areas with substantial well control, the seismic data is related to the well data so that the interpretation can be consistent with both. Seismic interpretation can be done both structurally and stratigraphically. Both types of interpretation are dependent on the resolution of the seismic reflection data. The higher the signal to noise (S/N) ratio of the data, the more reliable the seismic interpretation could be. Structural interpretation is the study of the geometry of reflectors on the basis of reflections times. This entails examining the seismic data, pickings of faults, mapping of reflections and posting the extracted information from the seismic section on the base map for the preparation of

accurate subsurface structural map which aids in the visualization of the subsurface geology. Stratigraphic interpretation involves delineating seismic sequences which represent different depositional units, recognizing seismic facies characteristics which suggest the depositional environment and analyzing reflection character variations to locate both stratigraphic changes and hydrocarbon accumulation (Sheriff and Geldart, 1995). Both structural and stratigraphic interpretation are complemented by seismic modeling where seismograms are synthesized from well information in order to derive insights into the physical significance of reflection events contained on seismic sections.

2.2.2 Nature of Seismic Waves

The seismic wave generated in the earth by a near- surface explosion of dynamite, mechanical impact, or vibration and so on is simply caused by the contrast in rock velocity and density. As the waves encounter each interface, they are either reflected or refracted according to the Snell's law (Fig.2.9). The reflected or refracted waves are detected by the array of geophones spread out on the surface of the earth. The reflection intensity or strength is determined by the contrast in product of velocity and density (acoustic impedance) between two adjacent rock

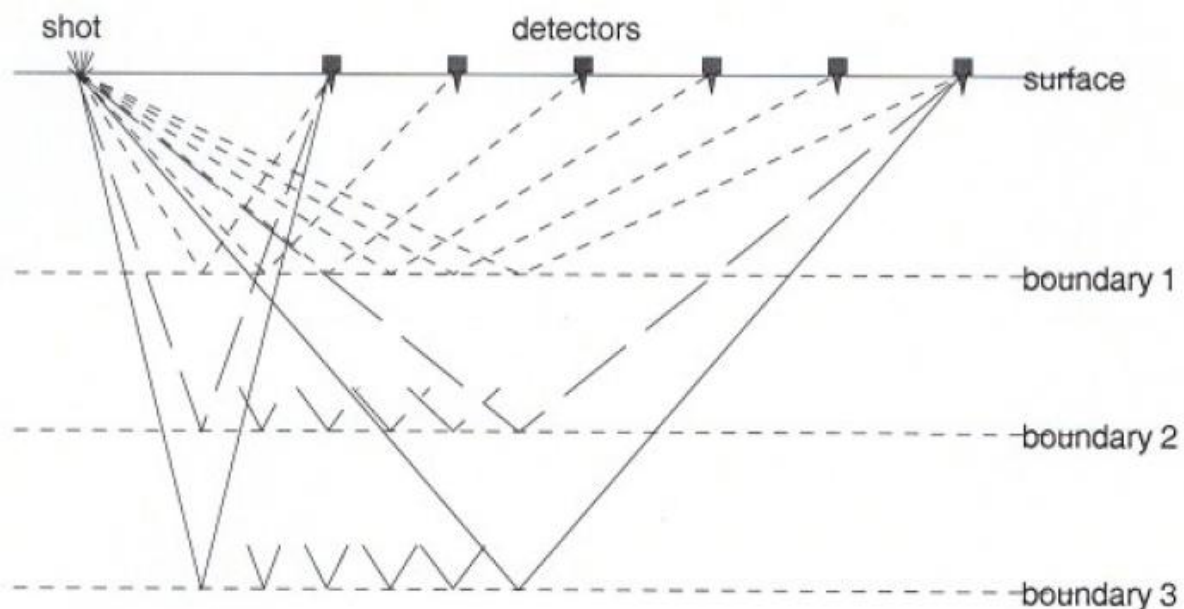


Figure 2.9: Diagram Showing Waves Detected by Various Geophones Reflected at Different Interfaces (After Dobrin and Savit, 1988).

An understanding of the properties of seismic waves and fundamentals of elasticity and the propagation of the waves in various media is required in order to discuss seismic exploration.

2.2.2.1 Types of Seismic Waves

Based on the movement of particles, three major types of seismic waves have been identified, which include longitudinal, transverse (body) and rayleigh waves. The last one is love waves which is a type of horizontally polarized transverse wave that combine with Rayleigh waves to constitute surface waves.

(1) Longitudinal Waves (P-Wave)

The movement of particle is in the same direction as that of the wave propagation (Figure 2.10a). Their amplitude decreases with offset from the shot points. The waves are regarded as compressional waves and are the fastest travelling waves required for seismic reflection and refraction prospecting.

(2) Transverse Waves (S-Wave)

The direction of particle motion within the transmitting medium is perpendicular to that of waves advancement (Figure 2.10b). When the motion is parallel to the surface they are described as (Sh) waves, and when in a vertical plane as (Sv) waves. Since deformation here is primarily a shearing motion, these waves are often referred to as shear waves. The waves are useful in the determination of elastic properties of rock though a great deal of research work has been carried out in oil industries with the purpose of putting them into more use (Dobrin and Savit; 1988).

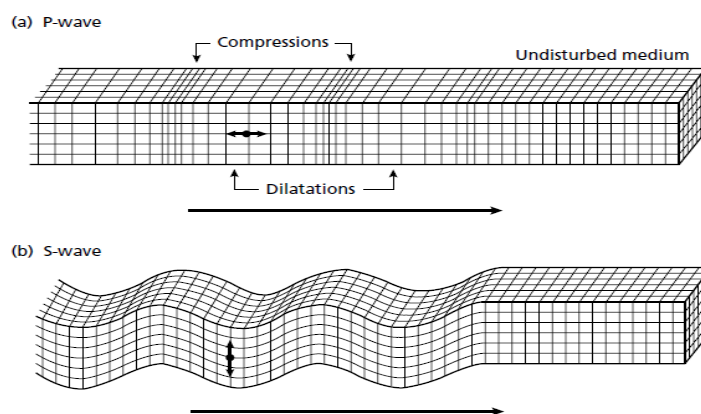


Figure 2.10: Elastic Deformations and Ground Particle Motions Associated with the Passage of Body Waves (a) P-waves (b) S-waves.(AfterDobrin and Savit; 1988).

(3) Rayleigh Waves

These waves spread out along the free surface with velocity lower than that of the compression and shear waves. The direction of particle motion is a retrograde ellipse with the major axis vertical and the minor axis in the direction of wave propagation (Figure 2.11a). The amplitude of the wave decreases exponentially with the depth below the surface. Seismologists have been able to derive useful information from the dispersive nature of the waves on earthquake records. They also constitute the major component of ground roll, a seismic noise which interferes with the strength and visibility of reflection on seismic records obtained in oil exploration.

(1) Love Waves

This is a type of horizontally polarized transverse (Sh) that occurs only when a low speed layer overlies a high speed substratum (Figure 2.11b). The velocity increases with wavelength, and the variation of velocity with frequency or wavelength is regarded as dispersion. Love waves are not recorded during seismic prospecting operations, where detectors are designed to respond mainly to vertical ground motion. However, they are used in earthquake seismology to study the earth near surface layering. Conclusively surface waves, rayleigh and love waves are inherently dispersive while longitudinal and transverse are non-dispersive.

In general,

$V_p > V_s > V_L > V_R$ in a given medium, where

V_p = Velocity of longitudinal waves, V_s = Velocity of transverse waves,

V_L = Velocity of love waves, and

V_R = Velocity of rayleigh waves

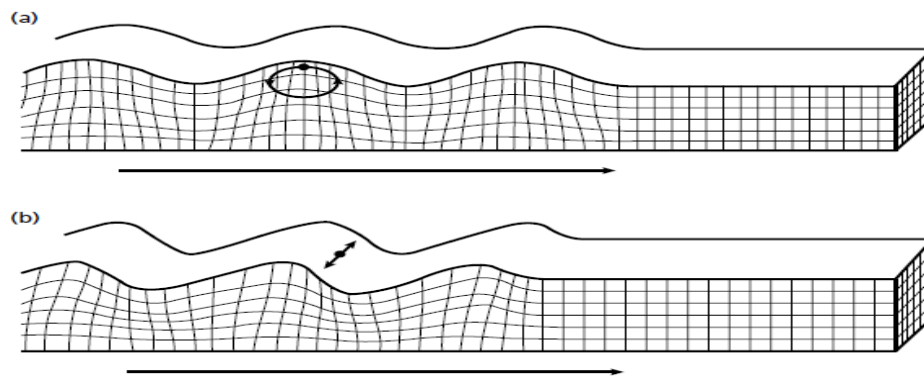


Figure 2.11: Elastic Deformations and Ground Particle Motions Associated with The Passage of Surface Waves (a) Rayleigh wave (b) Love wave (After Dobrin and Savit, 1988).

2.2.2.2 Wave Characteristics

Amplitude: This is the maximum displacement of wave particles.

Wavelength: Is the distance between adjacent peaks.

Velocity (V): The speed with which the waves move.

Frequency (F): Frequency and wavelength are related by this equation;

$$\text{Velocity} = \text{Wavelength} * \text{Frequency}.$$

However, the velocity and wavelength of seismic waves increase with depth in the earth whereas the frequency decreases.

(1) Propagation of Seismic Waves

Following an explosion, a spherical cavity is created with its periphery forming a zone of permanent deformation. However, at further distances away from the cavity, the seismic energy induces elastic deformation. The particle motion associated with its deformation can be described by the time-varying function. The physical basis for propagation of a wave is “Huygen principle”, which states that every point on an advancing wavefront is the envelop tangent to all secondary waves. The principle is used to describe reflection and refraction at layer boundaries and diffraction from sharp discontinuities.

(2) Wavelet

A wavelet is a seismic pulse with only a few cycles. Seismic signal which penetrates into the earth produces a large initial compression and also generates a tail of refraction and compression of increasing amplitude when refracted back at the interfaces. The whole of this sequence is involved in any reflection with the result that a weakly reflecting horizon may be swamped by the tail of a strong reflection from just above it. Through the process of deconvolution, the tail of the reflection is removed in order to make the signal as short as possible. The resulting simpler sequence of signal is called a wavelet. The two common wavelets are zero phases and minimum phase wavelets. Zero phase wavelet is symmetrical about the reflection time origin and has one strong wiggle with a much weaker opposite wiggle, while the minimum phase wavelet has a strong wiggle to one side.

2.2.2.3.1 Seismic Resolution

Reflecting interfaces are generally spaced much more closely than the wavelength of the embedded wavelet so that successive reflections overlap. Thus, resolution relates to how close two points can be and can yet still be distinguished. It is the process of separating the overlapping reflection effects. Hence, it allows for better identification of a reflection. Two types of resolution are considered. They are vertical and horizontal resolutions.

(1) Vertical resolution: From two reflections, one from the top and from the bottom of a thin layer, this is a limit on how close they are, yet are still separable. This limit depends on the thickness of the layer. The dominant wavelength of seismic wave is given by

$$\lambda = \frac{v}{f} \quad 2.1$$

Where, λ is the wavelength, V is the velocity and f is dominant frequency. The dominant frequency of seismic signal typically varies between 50Hz and 20Hz and increases with depth. Deconvolution tries to increase the vertical resolution by broadening the spectrum, thereby compressing the seismic wavelet. Since a wavelength determines resolution, deep features must be thicker than the shallow features to be resolved. The acceptable threshold for vertical resolution generally is a quarter of the dominant wavelength i.e. the limit of vertical resolution is a quarter of the dominant wavelength.

$$\lambda = \frac{\lambda}{4} \quad 2.2$$

The ability to resolve or detect small targets can be increased by increasing the dominant frequency of the stacked data.

(2) Horizontal Resolution

Horizontal resolution refers to how close two reflecting points can be situated horizontally, and yet can be recognized as two separated points rather than one. This can be determined by the fresnel zone, which is that portion of reflecting interface from which energy can arrive at a detecting station with a half-cycle so it can interfere constructively.

2.2.3 Seismic Data Processing

Seismic data processing involves manipulating data, usually to improve the signal to noise ratio so as to facilitate interpretation (Sheriff, 1984). The first objective of seismic data processing is the manipulation of the field data into the form of 2D seismic sections. The second objective is the manipulation of the seismic section into its migrated form in which dipping reflections have been moved to their correct positions in space. Processing operations include, applying corrections for unknown perturbing causes, rearranging the data, filtering it according to some criteria, measuring attributes, display and so on. In doing these, imperfections in the seismic source or in the seismic instrument and other signal distortions, which may occur in the earth, are compensated for. Seismic data processing is composed of basically five types of corrections and adjustment; time, amplitude, frequency phase content, data compressing (stacking), and data positioning (migration). These adjustments increase the signal- to- noise ratio, correct the data for various physical processes that obscure the desired (geologic) information of the seismic data and reduce the volume of data that must be analyzed by the geophysicist (Dobrin and Savit, 1988). Seismic data processing often follow a basic sequence that is varied to tailor to specific needs of the data (Sheriff and Geldart, 1995). Some of the processing in the sequence is optional and the sequence is sometimes changed or other processing added.

(1) Format Verification

This is the verification of the data arrangement after the field tapes have been received at the processing centre. This involves displaying the tapes magnetic pattern for the first few records on a print out and comparing with what is expected.

(2) Demultiplexing

Demultiplexing is the arrangement of the seismic data. The field data are written in a multiplexed format due to the way the sampling is done in the field. The first sample for each channel is recorded before the second sample for any channel. To create the output demultiplexed data set, the data samples for say shot 1, group 1 are assembled in the order of increasing time and output first, then the corresponding samples for shot 1, group 2 and so on and so forth.

(3) Editing

Editing is the detection of dead or exceptionally noisy traces. Noisy traces are zeroed and various quality checks are made on the data. Bad data are zeroed or are replaced with interpolated values. At this stage anomalously high amplitudes which are probably noise induced may be reduced to zero or to the level of the surrounding data. Traces are sometimes summed or arrays formed to reduce the data for further processing. Resampling also takes place if need be at this stage to make data less for future processing. A plot of each file shows what needs further editing and what type of noise attenuation are required. Near trace plot gives a quick look at the geological structure and for use in making decisions as to where velocity analyses are to be made. Near trace autocorrelation indicates multiple problems and aid in making deconvolution decisions.

(4) Common Midpoint Gather (CMP)

This is the sorting of traces with the same common-mid-point (CMP) into a CMP gather. Each gather contains many versions of the reflection information derived from different source- receiver pairs of a split spread. The reflections will be common from trace to trace of each gather. The traces of each gather are characterized by different reflections times due to the variations of offset.

(5) Seismic Datum Corrections

These are corrections applied to the seismic data to correct for the effect of topographic and near- surface irregularities, thus making the configuration of the subsurface not accurately represented by the section. The resulting section demonstrates a lack of event continuity as well as false structure. Datum correction or field statics include the elevation and weathering corrections. Static corrections are time adjustments. The correction is constant over time and shifts a whole trace.

(6) Normal Move Out (NMO) Corrections

Normal move out (NMO) corrections are time adjustments. Normal move out is a dynamic time correction which is a function of both time and offset and converts the times of the reflections into coincidence with those that would have been recorded if the source and receiver were located at the same point. The derived NMO equation, which is fundamental, is given as,

$$t^2 = t_0^2 + \left(\frac{x^2}{v^2} \right) \quad 2.3$$

Where;

x = Offset,

t_0 = Travel time at zero offset, when the source and receiver are in the same place,

v = velocity of the medium above the reflecting interface.

The NMO correction is effected by removing the amount of time from the reflection time. After correction, events line up or are flattened out on traces in the same common midpoint gather.

(7) Amplitude Adjustment

Amplitude adjustments correct the amplitude delay with time due to spherical divergence and energy dissipation in the earth. Spherical divergence is the decreases in wave strength with distance as a result of geometric spreading. The energy per unit surface area of the wave front (sphere) is inversely proportional to the square of the distance from the shot and also proportional to the square of the amplitude. Most of the delay due to spherical spreading occurs early, at times the amplitude of the reflection drops below the level of the ambient noise. The effect of spherical spreading is compensated for by compressing the amplitude of the earlier arrivals and amplifying those of the later ones. Trace normalization and trace balancing are also ways of adjusting amplitudes. Trace normalization is applied to the entire trace. It is directly applicable to the case of weak shots or a poor geophone plant. The combined effect is a section where the traces are uneven, across and down. Deep and weak reflections may be hard to see. Normalization enhances the appearance of continuity. Trace balancing is the adjustment of amplitudes within a trace. It effects is the suppression of

stronger arrivals coupled with the enhancement of weaker ones. Its goal is the improvement of even continuity and visual standout.

(8) Residual Statics

Residual statics are series of small, unsystematic errors in the original field static corrections. Their removal improves data continuity and interpretability. The corrections are performed on the move out corrected common midpoint gathers.

(9) Muting

Muting is the elimination of early arrivals, the first breaks to the geophone. The first breaks contain no reflected energy and therefore no information on the subsurface, because the seismic energy has found some near surface paths. Muting is done over certain time interval to keep ground roll, air waves or noise burst, out of the stack (Sheriff, 1984).

(10) Filtering

Filtering is the attenuation of certain components of a signal based on some measurable property. Filtering in most cases is done on the basis of frequency. The frequency-phase content of the data is manipulated to enhance signal and attenuate noise. Frequency filtering can be in the form of band pass, band- reflect, high pass (low- cut), or low- pass (high-cut) filters. Band pass filtering is used most because a seismic trace typically contains some low-frequency noise such as ground roll, and some high frequency ambient noise. Band pass filtering energy usually is confined to a bandwidth of approximately 10 to 70Hz, with a dominant frequency around 30Hz.

(11) Deconvolution

Deconvolution is the process of improving the temporal resolution of seismic data by compressing the basic seismic wavelet components and eliminating multiples leaving only the earth's reflectivity in the seismic traces. Before this process, the seismic section appears blurred and ringy but after correction it becomes finely detailed. Deconvolution also removes significant part of the multiple energy from the section.

(12) Migration

Migration is a process that moves dipping events in the up dip direction into their true subsurface position and collapse diffraction thereby delineating detailed subsurface features such as fault planes. The goal of migration is to make the stacked section appear similar to the geologic cross section along the seismic line (Yilmaz, 1987). The migration process gives clarity to the seismic section, the faults are easier to position and the derivation of a reliable time structure map becomes easier.

(13) Display

There are five conventional display modes in use. They are wiggles only, variable areas, wiggles with variable area, variable density and variable density with wiggles. A wiggle trace mode of display is a simple graph of amplitude against arrival times. In the variable area display, troughs of the wiggles are blank and the peaks are shaded black. One of the shortcomings of the variable area display is the difficulty in comparing the relative amplitudes of a peak and adjacent highs because of their difference. More so, interpreters are biased towards the black peaks thus neglecting the information in the troughs. The wiggle trace is treated to make the correlation between adjacent traces more visible. This is done by adding it to trough of the variable area resulting in the variable area with wiggle trace display. This display provides more information about the waveform, which may be of great importance of detailed studies.

2.2.4 Seismic Data Interpretation

After the processing of the seismic reflection data, interpretation can commence. This is the actual interpretation of the seismic section. The seismic section represents physical measurements of the subsurface displayed in two dimensions of space and time. In the course of interpretation, the data are carefully examined, faults picked, horizons mapped and seismic maps prepared.

2.2.4.1 Picking of Reflections

Reflections are picked based on the strength and continuities of the reflections. The same phase is followed from trace usually a peak or a trough, which indicates that the events are reflections from the same stratigraphic sequence. The strongest reflection usually results from unconformity or significant changes in lithology. Reflections also occur from minor changes in lithology (Sheriff, 1995).

2.2.4.2 Picking of Faults

A fault is a discontinuity of layers of rocks caused by the movement of the earth. After examining the seismic lines for quality, depth, reliable imaging and structural complexities, picking of faults commence. Since fault structures constitute one of the important hydrocarbon traps, it is necessary to delineate faults on seismic sections. The faults that were delineated during the course of study of this project were based on the following criteria;

- (1) Discontinuities in reflection
- (2) Displacement or distortion of reflection
- (3) Misclosures in tying reflections
- (4) Distortion or disappearance of reflection below suspected fault lines
- (5) Geologically real changes in dip near the fault.

2.2.4.3 Picking of Horizons

Horizon picking is one of the common activities involved in interpretation work. A horizon is a surface separating two different rock layers. The surface may be associated with a reflection, which can be carried over a large area (Sheriff, 1984). A prominent easily recognizable reflection is selected within the zone of interest and carried round the area to be mapped. The zone of interest is determined by either local geology or by selecting a prospective horizon from a well located in the area to be mapped. In a virgin area, it is best to select a horizon with strong reflectivity at an appreciable time. This work was carried out in an already explored area, thus borehole information was used.

2.2.4.4 Loop Tying

Loop tying involves transferring of features, particularly horizons and faults on inlines to the crosslines and vice-versa. The process serves two purposes;

- (1) It establishes a relationship between the traces of surfaces seen on seismic lines, and
- (2) It aids in projecting the horizons being mapped into areas where well control may not exist.

Loop tying also helps in tracing of horizons across the fault plane. Since horizons were first picked on inlines, the horizons were then transferred to the crosslines by loop tying. This was

done by first locating the points of intersection of the crossline on the inlines, and then the crosslines folded at the point of intersection and overlaid at the appropriate point of intersection on the inlines to effect correlations.

2.2.4.5 Timing and Posting of Horizons

Timing is done by reading reflection time on the horizon picked at convenient intervals. The time values obtained from this exercise are posted at appropriate points on the seismic situation map. The top and bottom of horizon picked were 0.2 milliseconds time interval. This represents the arrival time of the reflection from the sea level. The reflection times were posted on the respective shot points on the seismic situation map. In a similar way, faults were also posted to their corresponding locations on the base map. All the marked locations were then linked with thick smooth lines. Faults should be mapped before contouring since contour lines do not cross fault planes.

2.2.4.6 Time-to-Depth Conversion Curve

Seismic time-structure maps are usually converted to their corresponding depth maps because lateral velocity variations will give false time structures that may look like promising traps. In converting the time to depth, the time-depth (T-Z) conversion curve known as check shot survey could be used. This involves looking up the corresponding depth values to the posted time values in a time-depth graph that has been generated from checkshot data acquired from the evaluation phase drilling of a well or generated from the average of several stacking velocity functions that are close to a well (Coffen, 1984). Checkshot measures the actual time taken for a surface seismic source signal to travel to a receiver lowered down a well bore. Given maps of two-way-time to various horizons and of the average velocities between the formations, it is simple to multiply times by velocities to arrive at depth, building up the depth to each horizon in turn. These depth values can then be posted and contoured in the same ways as the two-way-time values. In practice, the amount of computation required if a large area is to be mapped on several horizons is formidable, and it is at this stage that a computer becomes extremely valuable. Various approaches can be used for the calculation of depth; the main problem is to make sure that the depth conversion is carried out in such a way to ensure consistency of values at line ties and near wells. One method is to represent the velocity data by a series of values on a square grid, the grid size being small enough to represent adequately the complexity of the data. Such grid can be constructed by reading off values by hand from the velocity contour maps, or can be machine-generated from the

contour map after the contours have been digitized. At each shot where depth conversion is required, the computer then calculates an average velocity value by interpolation from several neighbouring grid points, which is used in the depth calculation for that shot point. An advantage of this method is that well data can be included together with the grid points, and can be heavily weighted so that lines in the vicinity of wells will tie into them exactly.

2.2.4.7 Seismic Maps Generation

A seismic map is a contour map constructed from the seismic data. Values may either be time or depth, unmigrated or migrated with respect to a datum or with respect to another reflector (Sheriff, 1984). The interpretation of seismic maps is the foremost interpretation objective and the map is one of the primary tools employed in the search for hydrocarbons. Surface structure maps are usually constructed for the specific stratigraphic horizons to show in plan view the 3D geometric shapes of the horizon (Tearpock and Bischke, 1991). Seismic maps include isochron maps, isodepth maps, isopach maps, isovelocity maps and so on.

(1) Isochron Map

An Isochron map is a contour map of reflection time picked for a horizon at each shot point. Contained in isochron maps are structural information. Potential structural traps on these maps are characterized by closed structures as mapped on or near the surface of a reservoir rock formation (Macquillin, 1979).

Sheriff (1995) observed that the quantity of oil that can be trapped in the structure depends on the amount of closure, the area within the closing contour thickness and porosity of the reservoir beds. A closure is the property of a structure whereby it has a closing contour.

(2) Isodepth Map

Isodepth maps are maps showing contours of equal elevation. To prepare depth maps, the two-way travel times to the various horizons of interest are first depth-converted. Depth conversion can be performed directly from the root mean square velocities to the various horizons of interest by converting the two-way time to one-way and multiplying by their respective root mean square velocities at the velocity analysis point along the seismic section. Depth conversion can also be carried out using a time-depth graph (Tearpock and Bischke, 1991). This involves looking up the corresponding depth values to the posted time values in a time depth graph that has been generated from the checkshot data acquired the evaluation

phase of drilling a well or generated from the average of several stacking velocity functions that are close to a well (Coffen, 1984). Checkshot measures the actual time taken for a surface seismic source signal to travel to a receiver lowered down a well bore. Isodepth maps reveal the depositional topography of a field or an area. The primary dip of the field can be inferred from the map.

(3) Isopach Map

Isopach maps are contour maps denoting of equal thickness of a formation or group of formations and so on. According to Bishop and Num (1994), isopach maps are maps showing by means of a contour lines the distribution and thickness of a specific mapping unit. Isopach maps can be constructed by subtracting the time or depth values to two different horizons at each shot point or velocity analysis point and posting these values to the base map before contouring. Alternatively, they are often prepared by overlying maps of two different horizons and subtracting the contour values where the contours on one map cross the contour on the other. The differences are then recorded on a blank map and then contoured (Sheriff, 1995).

Isopach maps depict the thickness of sediments between horizons. These maps according to Sheriff (1995) show more than one period of movement of more than one rock unit. In discussing the interpretation of isopach maps, Sheriff (1995) noted that thickness trending towards a particular direction might indicate regional tilting downward in that direction during sedimentation or that the source of a folded competent bed indicates that the folding came after the deposition whereas deposition probably was contemporaneous with growth of an anticline if the thickness increases away from the crest. Isopach maps are used in studying the growth of structures and paleo-structures. They are also useful in assessing the geological history of an area particularly in unravelling the history of sediment deposition.

(4) Iso-velocity Maps

Iso-velocity maps are contour maps showing surfaces of constant seismic velocities (Sheriff, 1984). This iso-velocity map that is prepared is based on the information required. If the velocity of the interval between the picked horizons is the objective, then, an interval velocity map must be prepared. Interval velocity maps are prepared by posting the interval velocities computed at the velocity analysis points on to the base map and then contouring the values. According to Macquillin (1979), a particular rock interval exhibiting within a prospect lateral variation of velocity can be due to either change of lithology, in particular variation in

cementation and mineralogy or to tectonic effects. If it is due to tectonic effects it means that the interval must have been subjected to deeper burial in some places than others thus affecting porosity and velocity. Sheriff (1984) observed that in the absence of lithology, iso-velocity surfaces are likely to be nearly horizontal planes. However, where structural uplifts since change in velocity bend seismic rays and hence alter apparent structure.

2.2.5 Seismic Velocity

Seismic velocity is a vector quantity, which indicates the time rate of change of displacement. It is a property of the medium, which can be inferred from refraction time-distance curve, sonic logs, normal move out and in well shooting. Seismic velocities include; average, root mean square, stacking, instantaneous, interval and normal move out velocities. Seismic velocities are measured in boreholes through sonic logs and also by surface seismic data.

(1) Instantaneous Velocity (V_{INST})

Instantaneous velocity is the speed at any given moment of a wavefront in the direction of energy propagation. The instantaneous velocity, V_{INST} is defined as,

$$v_{inst} = \frac{dz}{dt} \quad 2.4$$

Where,

dz = Thickness of an infinitesimally thin layer

dt = infinitesimal time

Instantaneous velocity is used in seismic modeling.

(2) Average Velocity (V_{AV})

Average velocity (V_{AV}) is the average of all the interval velocities from the surface to the depth of a particular horizon. It is the ratio of the total depth of a reflecting surface below a datum and the observed total one- way reflection time from the datum to the surface. The average velocity, V_{AV} is defined as,

$$V_{av} = \frac{z1}{t1} + \frac{z2}{t2} + \frac{z3}{t3} + \frac{z4}{t4} + \dots + \frac{zn}{tn} \quad 2.5$$

Average velocity is measured during a well velocity survey of an interval or layer.

(3) Interval Velocity (V_{INT})

This is the average over some interval of travel path calculated from stacking velocities for the interval between reflectors where they are both horizontal. The interval velocity between two reflectors at depths z_1 and z_2 giving reflections having respective one – way times of t_1 and t_2 is defined as,

$$V_{int} = \frac{z_2}{t_2} - \frac{z_1}{t_1} \quad 2.6$$

The interval velocity is also called Dix velocity. It is given approximately as,

$$V_{in}^2 = \frac{v_{rms(n)}^2 T_n - v_{rms(n-1)}^2 T_{n-1}}{T_n - T_{n-1}} \quad 2.7$$

Where,

V_{in}^2 = Interval velocity between n^{th} and $(n-1)^{th}$ reflectors

$V_{rms(n)} V_{rms(n-1)}$ = Root – mean – square velocities (V_{RMS}) of the n^{th} and $(n-1)^{th}$ reflectors respectively.

$T_n T_{n-1}$ = Zero offset travel times for the n^{th} and $(n-1)^{th}$ reflectors respectively. Interval velocities are used in the identification of fluids (oil or gas), lithologies and tectonic. The accurate calculation of interval velocities from effective velocities could be achieved when the layers concerned are sufficiently thick.

(4) Stacking Velocity (V_{ST})

This is the velocity calculated from normal move out measurements and a constant velocity model (Sheriff, 1984). Stacking velocity (V_{ST}) is given as,

$$V_{st} = \frac{X^2}{T^2 - T_0^2} \quad 2.8$$

Where,

T = Travel time at X.

T_0 =Two way travel time (Echo time).

X = Distance (Variable separation of shot and receiver for a common reflection point sequence of shots.

Stacking velocity is used to maximize events in common midpoint (CMP) stacking and also for the computation of interval velocities for the interval between reflectors where they are both horizontal.

(5) Root Mean Square Velocity (V_{RMS})

Root mean square velocity V_{RMS} is not a physical measurable parameter. It is the result of a simple mathematical model. This mathematical model may be defined in geologic terms and may also be changed to fit reasonable or known geologic conditions.

Given a section consisting of horizontal layers with respective interval velocities of $V_1, V_2, V_3, \dots, V_n$ and one way interval times $t_1, t_2, t_3, \dots, t_n$, then the root mean square velocity is,

$$V_{RMS}^2 = V_1^2 t_1 + V_2^2 t_2 + \dots + \frac{V_n^2 t_n}{t_1 + t_2 + \dots + t_n}$$

The V_{RMS} is approximately the same as the V_{NMO} provided there is no dip on the beds. V_{RMS} may be used to determine interval velocities and also in depth conversion.

(6) Normal Moveout Velocity (V_{NMO})

Normal moveout velocity is the velocity implicit in the normal moveout correction applied before stacking. It is the velocity that provides the best fit to the observed moveout pattern at that zero offset time determined by a velocity analysis (Sheriff, 1984). Normal moveout velocity (V_{NMO}) is used to correct reflections for normal moveout (NMO), which enhances the reduction and stacking of common- mid- point (CMP) seismic data. For horizontal layers, normal moveout velocity (V_{NMO}) approximates the root- mean- square velocity V_{RMS} i.e.,

$$V_{NMO} \sim V_{RMS}$$

2.2.5.1 Factors Affecting Seismic Velocity

Seismic velocities are affected by several factors such as lithology, interstitial fluid, porosity, clay content, depth, density, temperature and so on. Lithology is an obvious factor affecting velocity however, velocity alone does not provide a good basis for distinguishing lithology because of the tremendous overlap of the velocity values of differing lithologies. Thus sand velocities can be lesser or greater than shale velocities. The presence and type of fluid in the interstices of rocks affect velocity a great deal. Varying amount of water, oil or gas fills these interstices. The replacement of water by oil or gas changes the bulk density and elastic constants and hence the P- wave velocity and reflection coefficient.

These changes according to Sheriff (1995) are sufficient to indicate the presence of oil or gas. Gas as a formation fluid is much more compressible than liquid and hence gas in pore spaces would lower the velocity much more than oil or water. Porosity generally decreases with increasing depth of burial (or overburden pressure) and hence velocity increases with depth. Porosity affects the velocity of the acoustic waves penetrating the rocks and as such, the higher the porosity, the lower the velocity. Han (1986) in their studies observed reduction of P- wave velocity when pores are clay filled while the S- waves velocity reduces by about 40%. Thus P- to S - wave velocity ratio in sandstone generally decreases as both porosity and clay content increases. This decrease according to Han (1986) is due to the ability of clay to significantly reduce the elastic moduli of the sandstone. Wang and Nun (1990) investigated the effect of temperature on the seismic velocities of hydrocarbon saturated rocks. They found that velocity decreases with increasing temperature the exact magnitude of which is dependent on the molecular weight of the hydrocarbon.

2.2.5.2 Relationship between Velocity and Porosity

Wyllie, etal., (1950), developed an equation for determining a rock's porosity viz;

$$\Delta t = \phi \Delta t_f + (1 - \phi) \Delta t_{ma} \quad 2.10$$

Where;

Δt = Specific transit time (slowness),

Δt_f = Specific transit time of the pore fluid,

Δt_{ma} = Specific transit time of the rock matrix, and

ϕ = Porosity

In terms of velocity, equation (10) can be re-written as,

$$\frac{1}{V} = (\phi) \frac{1}{V_f} + \frac{(1 - \phi)1}{v_{ma}} \quad 2.11$$

Where,

v = Bulk velocity

v_f = Velocity of the fluid

v_{ma} = Velocity of the rock matrix

Equations 2.10 and 2.11 are statistical and empirical. They make no allowance for the structure of a rock matrix, the connectivity of the pore spaces, or past history, all of which might be expected to affect velocity (Sheriff and Geldart, 1995).

2.3 SEISMIC ATTRIBUTES

Seismic attributes can be conveniently defined as “the quantities that are measured, computed or implied from the seismic data”. From the time of their introduction in early 1970’s seismic attributes gone a long way and they became a aid for geoscientists for reservoir characterization and also as a tool for quality control. Different authors introduced different kinds of attributes and their uses. With the introduction of 3-D seismic techniques and associated technologies and introduction of seismic sequence attributes, coherence technology in mid-1990’s, and spectral decomposition in late 1990’s has changed the seismic interpretation techniques and provided essential tools that were not available for geoscientists earlier. With the introduction of 3D visualization techniques, use of seismic attributes has attained a new dimension. Development of a wide variety of seismic attributes warrants a systematic classification. Also a systematic approach is needed to understand the use of each of these attributes and also their limitations under different circumstance.

2.3.1 Classification of Seismic Attributes

The Seismic Attributes are classified basically into two categories.

(1) Physical Attributes

(2) Geometric attributes

(1) Physical Attributes

Physical attributes are defined as those attributes which are directly related to the wave propagation, lithology and other parameters. These physical attributes can be further classified as post-stack and pre-stack attributes. Each of these has sub-classes as instantaneous and wavelet attributes. Instantaneous attributes are computed sample by sample and indicate continuous change of attributes along the time and space axis. The Wavelet

attributes, on the other hand represent characteristics of wavelet and their amplitude spectrum.

(2) Geometrical Attributes

The Geometrical attributes are dip, azimuth and discontinuity. The Dip attribute or amplitude of the data corresponds to the dip of the seismic events. Dip is useful in that it makes faults more discernible. The amplitude of the data on the azimuth attribute corresponds to the azimuth of the maximum dip direction of the seismic feature.

2.3.2 Post-Stack Attributes

Post stack attributes are derived from the stacked data. The Attribute is a result of the properties derived from the complex seismic signal. The concept of complex traces was first described by Tanner, 1979. The complex trace is defined as:

$$CT(t) = T(t) + iH(t) \quad 2.12$$

Where:

CT (t) = complex trace

T (t) = seismic trace

H (t) = Hilbert's transform of T (t)

H (t) is a 90° phase shift of T (t).

2.3.2.1 Signal Envelope (E) or Reflection Strength

The Signal Envelope (E) is calculated from the complex trace by the formula:

$$E(t) = \sqrt{T^2(t) + H^2(t)} \quad 2.13$$

The envelope is the envelope of the seismic signal. It has a low frequency appearance and only positive amplitudes. It often highlights main seismic features. The envelope represents the instantaneous energy of the signal and is proportional in its magnitude to the reflection coefficient. The envelope is useful in highlighting discontinuities, changes in lithology, faults, changes in deposition, tuning effect, and sequence boundaries. It is also proportional to reflectivity and therefore useful for analysing AVO anomalies. If there are two volumes that differ by constant phase shift only, their envelopes will be the same. This attribute is good for looking at packages of amplitudes. This attribute represent mainly the acoustic impedance Contrast, hence reflectivity. This attribute is mainly useful in identifying;

- (1) Bright spots
- (2) Gas accumulation

- (3) Sequence boundaries, major changes or depositional environments
- (4) Thin-bed tuning effects
- (5) Unconformities
- (6) Major changes of lithology
- (7) Local changes indicating faulting
- (8) Spatial correlation to porosity and other lithologic variations
- (9) Indicates the group, rather than phase component of seismic wave propagation

2.3.2.2 Envelope Derivative (RE)

This is the time derivative of the envelope.

$$RE(t) = DE(t)/DT \quad 2.14$$

The derivative of envelope highlights the

- (1) Change in reflectivity and is also related to the absorption of energy.
- (2) Sharpness of the rise time relates to absorption
- (3) Sharp interfaces
- (4) Shows discontinuities

It is used in computation of group propagation direction. When compared with phase propagation direction, it may indicate dispersive waves.

2.3.2.3 Second Derivative of Envelope (DDE)

This is given by:

$$DDE(t) = d^2E(t)/dt^2 \quad 2.15$$

The second derivative of the envelope highlights the interfaces very well - the places of change. This attribute is not too sensitive to the amplitude and can highlight even weak events, shows all reflecting interfaces visible within seismic band-width

- (1) Shows sharpness of events
- (2) Indicates sharp changes of lithology
- (3) Large changes of the depositional environment, even corresponding envelope amplitude may be low.
- (4) Very good presentation of image of the subsurface within the seismic bandwidth.

2.3.2.4 Instantaneous Phase

Instantaneous phase attribute is given by

$$\phi(t) = \arctan [H(t)/T(t)] \quad 2.16$$

The seismic trace $T(t)$ and its Hilbert transform $H(t)$ are related to the envelope $E(t)$ and the phase $\phi(t)$ by the following relation

$$T(t) = E(t) \cos(\phi(t)) \quad 2.17$$

$$H(t) = E(t) \sin(\phi(t)) \quad 2.18$$

Instantaneous phase is measured in degrees $(-\pi, \pi)$. It is independent of amplitude and shows continuity and discontinuity of events. It shows bedding very well. Phase along horizon should not change in principle, changes can arise if there is a picking problem, or if the layer changes laterally due to “sink-holes” or other phenomena. This attribute is useful as

- (1) Best indicator of lateral continuity,
 - (2) Relates to the phase component of the wave-propagation.
 - (3) Can be used to compute the phase velocity,
 - (4) Has no amplitude information, hence all events are represented,
 - (5) Shows discontinuities, but may not be the best. It is better to show continuities
- Sequence boundaries,
- (6) Detailed visualization of bedding configurations,
 - (7) Used in computation of instantaneous frequency and acceleration.

2.3.3 Pre-Stack Attributes

RMS velocities of reflectors

This may be Time Migration velocity analysis, independent of major influence of dips. This is used for sand/shale ratios estimation, high pressure shale zone detection, major lithologic change detection, and etc.

- (1) Zero offset pressure-wave seismic section.
- (2) Zero offset shear-wave seismic section estimation.
- (3) Group velocity, phase velocity decomposition.
- (4) Trace envelope amplitude variation with respect to offset.
- (5) Instantaneous frequency variation with respect to offsets.

2.4 WELL LOGGING

After seismic survey has been carried out and interpretation of data has been done to ascertain a hydrocarbon bearing reservoir at a particular depth, a well is drilled. Information

is then deduced about the formation encountered in the drilled hole and these are recorded as a function of depth on logs. A log is therefore any graphic representation of variations in one parameter versus another, generally depth. Wireline logs are measurements of physical parameters in the formation penetrated by the borehole. The records obtained are displayed in form of curves.

2.4.1 Open Hole Analysis

There are two ways in which open hole can be logged.

- (1) Wireline logging: In this case, logging is done at another time after a section of the hole has been drilled.
- (2) Logging while drilling (LWD). Here, measurements or logging are done at the same time when the hole is being drilled. It is also called measurements while drilling (MWD). The two differ in that one is run during drilling while the other is run at a later time. The logs curve are interpreted so as to;
 - (1) Identify porous and permeable zones
 - (2) Porosity estimation
 - (3) Water saturation calculation
 - (4) Differentiation between oil and gas sections
 - (5) Perform basic formation evaluation.

In other to do these, specific logs tools are used. Table 2.1 below shows the open hole logging tools, measurements and uses.

2.4.2 Basic Well Log Classification

Logs can be classified according to their uses.

1. Lithology Log

The lithology log is usually on the first track of the log. It is used to identify reservoir rock from non-reservoir. i.e sandstone and shale. Tools used for lithology log include:

Gamma ray (GR): The gamma ray log is a measurement of the natural radioactivity of formations. Gamma ray is bursts of high energy electromagnetic waves. Some elements in nature emit gamma radiation. Nearly all gamma radiation are emitted by Potassium (K), Thorium (Th) and Uranium (U) elements common in the earth's crust. Generally reservoir rocks like Sandstone, Limestone and Dolomite contains none or only small amounts of these elements and therefore have low gamma radiation levels. Some other

rock types like Shale, Sylvite have large amounts of potassium and thorium. The resulting high gamma ray radiation level contrast with the low gamma ray levels of the adjacent

Table 2.1: Type of Well Logs that are Commonly Used in Formation Evaluation (SPDC 1992).

Log	Property Measured	Units	Geological Interpretation
Spontaneous potential	Natural electric potential (relative to drilling mud)	Millivolts	Lithology, correlation, curve shape analysis, porosity
Conventional resistivity	Resistance to electric current flow	Ohm-metres	Identification of coal, bentonites, fluid types
Micro-resistivity	Resistance to electric current flow	Ohm-metres and degree	Borehole imaging, virtual core
Gamma ray	Natural radioactivity (K, Th, U)	API units	Lithology (including bentonites, coal), correlation, shape analysis
Sonic	Velocity of compressional sound wave	Microseconds/metre	Identification of porous zones, tightly cemented zones, coal
Neutron	Hydrogen concentration in pores (water, hydrocarbons)	Percent porosity	Porous zones, cross plots with sonic and density for lithology
Density	Bulk density (electron density) includes pore fluid in measurement	Kilograms per cubic metre	Lithologies such as evaporates and compacted carbonates
Dipmeter	Orientation of dipping surfaces by resistivity changes	Degrees (azimuth and inclination)	Paleo flow (in oriented core), stratigraphic, structural analyses
Caliper	Borehole diameter	Centimetres	Borehole state, reliability of logs

Reservoir formations. The gamma ray tool consists of a single gamma ray detector, which records natural gamma radiation against depth. The total gamma ray level is recorded and plotted in API Units on a scale of 0-150 API.

The gamma ray is important in that it;

- (1) delineates between reservoir and non-reservoir
- (2) evaluate reservoir quality –Net/Gross
- (3) estimate the shaliness of reservoir rock
- (4) Helps in correlating reservoirs between wells based on their gamma ray signatures.

(a) Evaluation Technique of Gamma Ray Log

The interval of interest should consist of reservoir rock and shale layer only. Within this interval, the gamma ray level of thick shale bed(s) is read. This reading is assumed to represent 100% shale. A straight line through these points is called the shale-line. Similarly a sand-line is constructed by reading the average gamma ray level of thick clean sands, thus sands with the lowest gamma ray level. A near vertical line in the middle between the shale and the sand lines is called the cut-off line. All intervals where the gamma ray log is on left of this cut off line is then assumed to be reservoir. The level of gamma ray within a reservoir interval is a measure of its shaliness.

(1) Self-Potential (SP) Log: The SP log measures the flow of current induced by changes in salinity between drilling and formation fluids. The self-potential log resembles the gamma ray log in that both respond to the presence of clay. The gamma ray log responds to radioactive elements in the clay while the self-potential log responds to the electrochemical effect created by the negative surface charge of clay particles. In situations where the reservoirs in a well contain some radioactive elements a self-potential log is run as an alternative to a gamma ray log. Apart from its ability to differentiate lithologies, the self-potential log is also used to estimate formation water resistivity, estimate shaliness of a formation and correlate geological information between wells.

2.4.2.2 Porosity Log

Porosity log is the primary source of reservoir volume information. It is usually found on the third track of the log and it is used to determine fluid type and fluid contacts at respective depths. The following are the tools employed for this;

(1) Sonic log: This uses various forms of sound wave propagation. The acoustic logging principle is related to seismic exploration methods, since both derive data from wave travel times. This log measures velocity of a sound wave through rock medium which is dependent upon the lithology and the porosity. The basic acoustic log is a recording versus depth of the time (dt). This requires compressional sound waves to travel one foot of formation, known as interval transit time. The interval travel transit time for a given formation depends on its lithology and porosity. Dependence on porosity when lithology is known makes the acoustic log very useful in formation evaluation.

(2) Density log

Since the density of a mixture of components is a linear function of the densities of its individual constituents, it is easy to calculate the porosity of a porous rock reservoir rock. Reservoir rock consists of rock matrix (e.g quartz, calcite, and dolomite) and pore fluid (e.g water, oil, gas). The bulk density (p_b) of a reservoir rock is the weighted average density of the pore fluid(s) (p_f) and its rock matrix (p_{ma}). To calculate fractional porosities, the expression can be given as follows;

$$\Phi_D = \frac{p_{ma} - p_b}{p_{ma} - p_f} \quad 2.19$$

Where

p_b = Bulk density

p_{ma} = Matrix density

p_f = Fluid density.

(3) Neutron log

Neutron log is a fundamental particle found in the nucleus of all atom except hydrogen which contain only a proton. Neutron penetrate through brick walls and steel plates with greatest ease because the neutron has approximately the same mass as the proton, but carries no electrical charge. The neutron log contains a radioactive source of fast neutrons with thermal neutron detectors at a fixed distance from source. In the presence of hydrogen (water) the neutron loses most of its energy and thus counts rates of the neutron arriving at the detectors which are inversely related to the water content or water filled porosity.

(4) Neutron/Density Log Combination

The combination of neutron and density logs is mainly to distinguish between oil and gas bearing zones. Both the density and Neutron tools determine the porosity of a reservoir, but they do this by measuring different quantities. The density tool measures the bulk density, while the neutron measures the hydrogen density. For this reason, both tools respond differently to some pore fluids and lithologies. It is standard practice to plot both logs in one track, using a scale such that both logs overlay in water bearing limestone. Using these scales, the logs will separately uniquely in other lithologies and pore fluids. For example

- (1) In gas bearing reservoirs the recorded neutron porosity is lower and the bulk density is reduced, compared with the responses in a similar water/oil bearing formation. These effects can be significant, depending on the gas situation in the invaded zone. The

resulting large separation with neutron on the right and density on the left is called gas separation.

- (2) Shales have an inverted effect (shale separation). Due to the clay-bound water, which is chemically attached to the clay particles, the neutron tool records high porosity, where in reality no effective porosity is present.

2.4.3.3 Resistivity Log

There are two main types of resistivity measuring devices, Dual laterologs (DLL) and the Dual induction logs (DIL). The true formation resistivity must be measured to be able to evaluate the hydrocarbon saturation in the reservoir. When the resistivity measurement is carried out by a sonde in the borehole, the measurement will be influenced by the mud filtrate that has invaded the formation. Three independent resistivity measurements are required to eliminate the effect of the invaded zone and determine the true formation resistivity. These measurements are the deep, the shallow and the MSFL, each having a different depth of investigation.

- (1) LLD looks deep into the reservoir and measures the true formation resistivity. The LLD is hardly influenced by the borehole, mudcake and invaded zone. It will usually read the resistivity of the uninvaded reservoir rock (R_o or R_t).
- (2) LLS look shallow into the reservoir and measures the invaded zone resistivity. The LLS is significantly influenced by the borehole, mudcake and invaded zone. It can be used to correct the LLD where necessary.
- (3) MSFL reads the resistivity of the invaded reservoir rock (R_{xo}) close to the well bore for non-reservoir, because of the lack of permeability in non-reservoir rock.

All the three resistivity devices will therefore read the same resistivity for the reservoirs, if the reservoirs are porous; mud filtrate resistivity (R_{mf}) will invade the zone close to the wellbore replacing all the formation water resistivity (R_w) and part of the hydrocarbon present.

2.5 PETROPHYSICAL ANALYSIS

Formation evaluation which is the process of using geophysical measurements to evaluate the characteristics of subsurface formations is an aspect which deals with the physical

properties of rock and fluid content in them. Although formation evaluation covers a very large range of measurements and analytical techniques, it plays a significant role by identifying and evaluating different lithologies or formations, detecting potential reservoirs, fluid type, contacts and estimation of reserves. Petrophysics can therefore be defined as a term used to express the physical and chemical properties of rocks which are related to pore and fluid distributions particularly as they pertain to the detection and evaluation of hydrocarbon bearing reservoirs.

2.5.1 Fundamental of Petrophysical Parameters

The properties of primary concern are;

- (1) Porosity: Porosity is defined as the pore volume per unit volume of rock or the fraction of the volume not occupied by rock matrix. It is usually denoted by (Φ) and expressed in fraction or percentage. In reservoir rocks we can identify two types of porosity; primary and secondary porosity. Primary porosity is the original pore space of the rock from where it was deposited and secondary porosity such as vugs is caused by post depositional process such as tectonic forces or by formation water flows. Consolidated sandstone of Niger Delta usually have porosities in the range of 22-28%, while the unconsolidated sands of the Niger Delta may have porosities of 30% or higher. Table 2.2 below shows the range of porosity value.
- (2) Netpay: This is the thickness of reservoir containing hydrocarbon. It is measured from well logs.
- (3) Fluid Saturation: Saturation of a reservoir is that portion of its pore volume that is occupied by the fluid considered. In petrophysics or formation evaluation water saturation (S_w) is mostly considered as the standard. Thus it is that percentage of pore volume that contains water. Water saturation is said to be 100% if water is the only fluid present in the rock. The hydrocarbon saturation is that portion of the pore volume not occupied by the formation water or water saturation (S_w). Thus it can be calculated as $100-S_w$. Water saturation will never be zero because under normal condition, no pressure will be high enough to displace all the water in the pore spaces. This residual water is known as connate water. The same applies to drained hydrocarbon reservoir, there will always be some hydrocarbon that remains in the pore spaces. This is called the residual oil and gas of the rock. All these petrophysical parameters are deduced from the well log data.

Table 2.2: Classification of porosity in the study area (Short and Stauble 1967)

RANGE (%)	STATE
0-5	Negligible
5-10	Poor
10-15	Fair
15-20	Good
20-25	Very good
>25	Excellent

CHAPTER THREE: MATERIALS AND METHODS

3.1 Materials

The data set used in this research project were acquired through MONI PULO PETROLEUM LIMITED which includes 3-D seismic reflection data, suites of composite logs from four wells and check shot data over the field of interest. Petrel (seismic to simulation software) 2010 version was used for the project.

3.1.1 3-D Seismic Section

The 3-D seismic reflection data comprising 274 in-lines and 256 cross-lines which cover an area of 74 km² were utilized for this research work. The reflection quality of the data is very good and faults and stratigraphic picks for the horizons are easily recognizable.

3.1.2 Geophysical Well Logs

Four vertical wells, which include well 2, well 7, well 9 and well 11, were drilled in the field of study for hydrocarbon exploration and exploitation (Figure 3.1). The wells were logged at different depths utilizing a variety of logs (Tables 3.1).

3.1.3 Velocity Check Shot Survey Data

The check shot is used to determine velocity that will apply to a seismic section by using a technique similar to that used in making sections. Shootings are fired near the surface of the ground and recording is made from a geophone at known depths in the well. Thus, travel time from the surface down to formations is measured. The data obtained from the check shot used for the time–depth conversion and to generate synthetic seismogram for seismic to well tie.

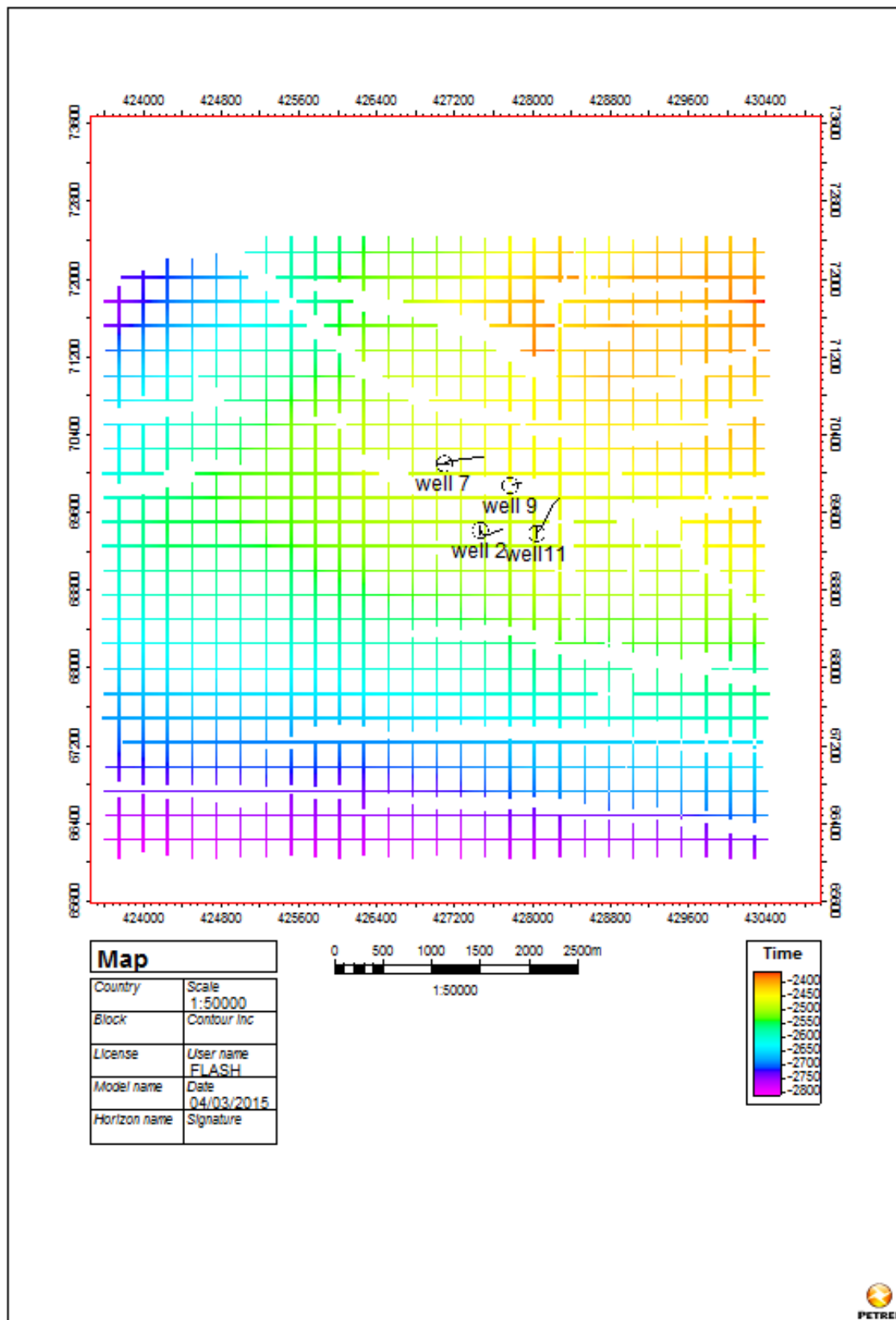


Figure 3.1 Base map Showing the Locations of Wells and NW-SE Direction of Correlation.

Table 3.1: Geophysical Wireline Logs of the Study Area

Well No/Well Log	Log Type	W-2	W-7	W-11
Lithology Logs	GR	++	++	++
	SP	++	++	++
Resistivity Logs	Laterolog	--	--	--
	Lateral	--	--	--
	Short Normal	--	--	--
	Long Normal	++	++	++
	Spherical Focussed	--	--	--
	Medium Induction	--	--	--
	Deep Induction	--	--	--
Porosity Log	Sonic	++	++	++
	Neutron	++	++	++
Caliper		++	--	--

++ Available -- Not Available

Table 3.1 depicts the corresponding time to depth curves generated from the digital data.

3.2 METHODS OF STUDY

The methodology utilized in this thesis is broken into three basic phases: structural interpretation, seismic attributes and petrophysical analysis.

3.2.1 Structural Interpretation

Fault picking was done on the vertical seismic display across the whole seismic volume. Seismic to well tie was done to match events on well logs to the specific seismic reflections with the aid of checkshot. Horizons were picked on the seismic section, auto tracked and the horizon surfaces were converted to obtain the time structure maps. The time structure maps were converted to depth structure maps using the checkshot data provided (fig 3.2).

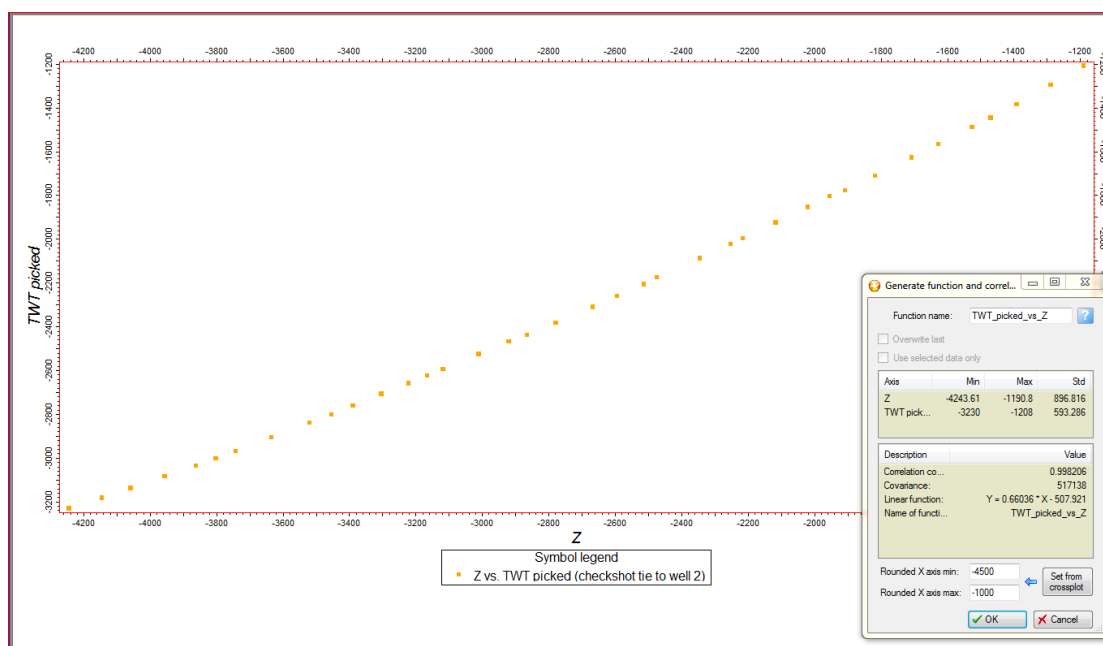


Fig. 3.2: Time to Depth Conversion Curves and linear function from the check shot of well 2

3.2.2 Seismic Attributes

In order to enhance the hydrocarbon potential of the field, seismic attribute analysis was carried out where Attributes derived from surface maps were integrated with rock properties to map the surfaces away from the wells into the field covered by the seismic. Using three surface attributes time map which are Upper Loop Area, Interval Average and Root Mean Square (RMS). These attribute maps were generated to find anomalies, hence delineating the lateral extent of the reservoirs of interest, also to reveal stratigraphic traps and depositional environment like channels, pinchouts etc.

3.2.3 Petrophysical Analysis

This involves the use of empirical formulae to estimate the petrophysical properties of the mapped reservoir units delineated on the well logs. The reservoir units which was identified through the use of the electrofacies signatures were further characterized quantitatively to arrive at these petrophysical parameters, which includes: volume of shale, formation factor, porosity, water saturation, permeability and so on. Some of these parameters are discussed below:

3.2.3.1 Gamma Ray Index

The gamma ray log was used to determining the gamma ray index using the formula according to Asquith and Gibson, 1982:

$$I_{GR} = (GR_{LOG} - GR_{MIN}) / (GR_{MAX} - GR_{MIN}) \quad \dots\dots\dots 2.1$$

Where,

- I_{GR} = gamma ray index
- GR_{LOG} = gamma ray reading of formation from log
- GR_{MIN} = minimum gamma ray (clean sand)
- GR_{MAX} = maximum gamma ray (shale)

3.2.3.2 Volume of Shale

The volume of shale was calculated by applying the gamma ray index in the appropriate volume of shale equation according to Larionov (1969) for tertiary rocks:

$$V_{sh} = 0.083[2^{(3.7 \times IGR)} - 1.0] \quad \dots\dots\dots 2.2$$

Where, V_{sh} = volume of shale I_{GR} = gamma ray index.

3.2.3.3 Porosity

The computation of porosity was done in stages, the first involved the use of the Wyllie equation to estimate the density derived porosity (ϕ_D), and then the neutron-density porosity (ϕ_{N-D}), was estimated using the neutron (ϕ_N) porosity coupled with the density derived porosity. The Wyllie equation for density derived porosity is given as:

$$\phi_D = (\ell_{max} - \ell_b) / (\ell_{max} - \ell_{fluid}) \quad \dots\dots\dots 2.3$$

where:

ℓ_{max} = density of rock matrix = 2.65 g/cc

ℓ_b = bulk density from log

ℓ_{fluid} = density of fluid occupying pore spaces (0.74g/cc for gas, 0.9g/cc for oil and 1.1 g/cc for water).

The Neutron – Density porosity could be calculated according to Shell/Schlumberger (1999) as:

$$\phi_{N-D} = (\phi_N + \phi_D)/2 \quad \text{for oil and water column} \quad 2.4$$

$$\phi_{N-D} = (2 \phi_D + \phi_N)/3 \quad \text{for gas bearing zones} \quad 2.5$$

3.2.3.4 Formation Factor

This was achieved using the Humble equation:

$$F = a/\phi^m \quad 2.6$$

Where,

F = formation factor

a = tortuosity factor = 0.62

ϕ = porosity

m = cementation factor = 2.15

3.2.3.5 Formation Water Resistivity (Ωm)

Using the Archie's equation that related the formation factor (F) to the resistivity of a formation at 100% water saturation (R_o) and the resistivity of formation water (R_w), the resistivity of the formation water was estimated as:

$$R_w = R_o/F \quad 2.7$$

3.2.3.6 Water Saturation

Determination of the water saturation for the uninvaded zone was achieved using the Archie (1942) equation given below.

$$S_w^2 = (F \times R_w)/R_T \quad 2.8$$

$$\text{But, } F = R_o/R_w \quad 2.9$$

Thus,

$$S_w^2 = R_o / R_T \quad 2.10$$

Where,

S_w = water saturation of the uninvaded zone

R_o = resistivity of formation at 100% water saturation

R_T = true formation resistivity

3.2.3.7 Hydrocarbon Saturation

This was obtained directly by subtracting the percentage of water saturation from 100.

Thus $S_{hy} = 1 - S_w$

Or $S_{hy} \% = 100 - S_w \%$

2.11

Where, S_{hy} is the hydrocarbon saturation (expressed as a fraction or as percentage).

3.2.3.8 Resistivity Index

This was estimated using the ratio of formation true resistivity (R_t) to resistivity of formation at 100% saturation (R_o):

$$I = R_t / R_o \quad 2.12$$

Where, I is the resistivity index, When I is equal to unity, it implies that the reservoir is at one hundred percent (100%) water saturation, The higher the value of I , the greater the percentage of hydrocarbon saturation.

3.2.3.9 Bulk Volume Water

Bulk volume of water (BVW) was estimated as the product of water saturation (S_w) of the uninvaded zone and porosity (ϕ_{N-D}).

Thus,

$$BVW = S_w \times \emptyset_{N-D} \quad 2.13$$

Where,

\emptyset_{N-D} = neutron-density porosity.

3.2.3.10 Hydrocarbon Pore Volume

The hydrocarbon pore volume (HCPV) is the fraction of the reservoir volume occupied by hydrocarbon. This was calculated as the product of neutron-density porosity and hydrocarbon saturation as shown below:

$$HCPV = \emptyset_{N-D} \times (1 - S_w) \quad 2.14$$

$$HCPV = \emptyset_{N-D} \times (S_h)$$

3.2.3.9 Irreducible Water Saturation

The irreducible water saturation was calculated using the following relationship:

$$S_{wi} = (F/2000)^{1/2} \quad 2.15$$

Where,

S_{wi} = irreducible water saturation

F = formation factor.

However, this theoretical estimate of irreducible water is majorly useful in the estimation of relative permeability.

3.2.3.11 Permeability

This was based on the relationship between permeability, porosity, and irreducible water saturation according to Wyllie and Rose, (1950). The relationship is expressed as:

$$K = [(250 \times (\emptyset_{N-D})^3)/S_{wi}]^2 \quad 2.16$$

3.2.3.12 Shaliness (V_{sh} Total)

This is the total volume of shale represented as a depth factor within a well. It is calculated by:

$$\text{Average } V_{sh} \times \text{Gross thickness} \quad 2.17$$

3.2.3.13 Net Thickness

This is the column of the reservoir that is occupied by reservoir formation (e.g. sand) only and exclusive of non-reservoir formations (e.g. shale). It is calculated by:

$$\text{Gross Thickness} - V_{sh} \text{ Total} \quad 2.18$$

3.2.3.14 Net to Gross Ratio

This is the ratio between the net reservoir thickness and the gross reservoir thickness. However in terms of hydrocarbon pay, it could be calculated as the ratio between the net pay thickness and the gross pay thickness.

$$\text{NTG} = \text{Net thickness} \div \text{Gross Thickness} \quad 2.19$$

3.2.3.15 Effective Porosity

This is the porosity of the interconnected pore spaces. It assumes the absence of shale from the reservoir. It can be calculated using the following relationship:

$$\Phi_{\text{effective}} = (1 - V_{\text{SHALE}}) * \phi_{N-D} \quad 2.20$$

3.2.3.16 Storage Volume

This is the capacity to store hydrocarbon in the reservoir. The storage volume is always higher than the hydrocarbon pore volume within a well because the net pay zone is inclusive of the grain matrix whereas, the grain matrix is absent in the hydrocarbon pore volume computation as only the hydrocarbon in the pore spaces is calculated for,

$$\text{Storage Volume} = \phi_{N-D} * \text{Net Pay Thickness} \quad 2.21$$

3.2.3.17 Volume of Oil Resources

This is the volume of oil resources per unit acre in a field. It could be used to estimate oil reserve volume in the field.

$$\text{Volume of Oil Resources} = (7758 * h * HCPV) / B_o \quad 2.22$$

Where h = net pay oil, B_o = Formation oil volume factor = 1.2 bbls/STB

3.2.3.18 Volume of Gas Resources

This is the volume of gas resources per unit acre in a field. It could be used to estimate gas reserve volume in the field.

$$\text{Volume of Gas Resources} = (43560 * h * HCPV) / B_g \quad 2.23$$

Where

h = net pay gas, B_g = Formation gas volume factor = 0.005 cuft/scf

3.2.3.19 Volume of Oil Originally in Place

Oil originally in place is computed with the following equation:

$$OOIP = \text{Volume of Oil Resources} * \text{Area covered by oil} \quad 2.24$$

Here, recovery factors have not been applied. This volume could be calculated directly from the volume of oil resources contour map. The area of the map occupied by oil is calculated sectionally with respect to the contour intervals. The individual area is then multiplied by the individual contour value to get the individual volumes. Finally, all the individual volumes are added to get the total volume of oil resources in the field which is equivalent to the volume of oil in place. The unit here is stock tank barrels.

3.2.3.20 Volume of Gas Originally in Place

This is calculated the same way as that of oil originally in place from the volume of gas resources contour map. The unit here is standard cubic feet.

$$GOIP = \text{Volume of Gas Resources} * \text{Area covered by gas} \quad 2.25$$

3.2.3.21 Direct Measurement of Hydrocarbon in Place

The hydrocarbon originally in place could also be computed directly using the average value for the net pay thicknesses, average hydrocarbon saturations and average porosity values and substituted in the following equations:

$$OOIP = (7758 * A_{oil} * h_{oil} * s_{h(oil)} * \phi_{N-D}) / b_o \quad 2.26$$

$$OGIP = (43560 * A_{gas} * h_{gas} * s_{h(gas)} * \phi_{N-D}) / b_g \quad 2.27$$

A_{oil} = Area occupied by oil, A_{gas} = Area occupied by gas, h_{oil} = Average height of oil column, h_{gas} = Average height of gas column, $s_{h(oil)}$ = Hydrocarbon saturation (oil column) and $s_{h(gas)}$ = Hydrocarbon saturation (gas).

CHAPTER FOUR: RESULT PRESENTATION, INTERPRETATION AND DISCUSSION

4.1 RESERVOIR MAPPING:

Figure 4.1 depicts the well correlation panel of well 2, well 11, well 9 and well 7 in the Northwest-Southeast direction. The suites of the log associated with these well are gamma ray log, resistivity log, Neutron-porosity log and density log. Gamma ray log which is a lithology log was used for lithologic differentiation between porous and non porous formation, Resistivity log was used to delineate hydrocarbon bearing zones from water zones while both Neutron and Density log was used to delineate oil and gas contact. Two reservoirs at 3430ft and 3544ft as top of Sand A and Sand B(thicker reservoir) were mapped . The reason for this was to investigate the presence of hydrocarbon at the location of each of the wells, which is a guide to lateral distribution of the reservoirs

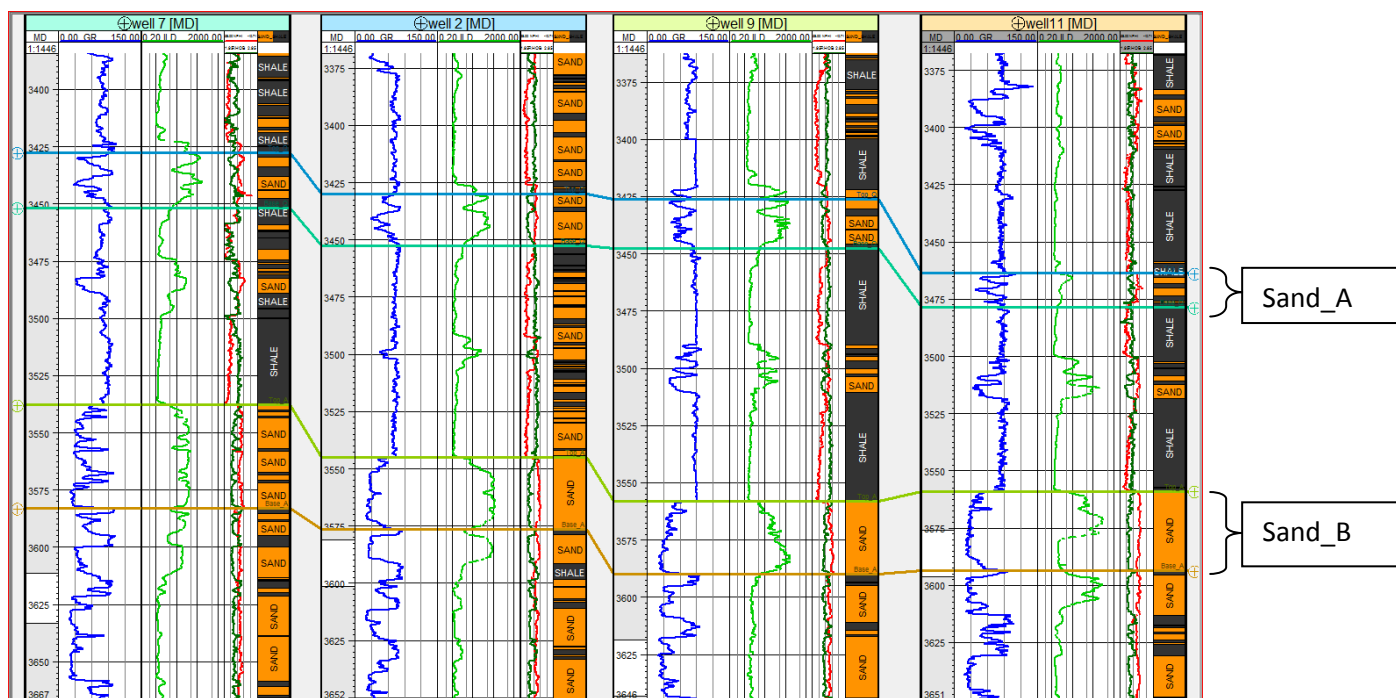


Fig.4.1 Well logs from well 2, well 7, well 9, well 11 wells showing the delineated Reservoirs (Sand_A and Sand_B) with Gamma ray, Resistivity and the porosity logs

4.2 FAULT INTERPRETATION AND HORIZON MAPPING.

Figure 4.2 Well to seismic tie revealed good tie of the 3D seismic of the reservoirs at well 2 depicts the mapped fault and horizon on the seismic section of inline 5717. Seven faults labelled F1, F2, F3, F4, F5, F6, and F7 were mapped, and Structures with multiple growth (listric) faults and collapsed crest structure, which is in conformity with the structural geometry of the Niger Delta. Four horizons were mapped (H1, H2, H3 and H4), bright spots reflections were observed as horizon picking was done. The horizons depict the top and base of the two reservoirs (Sand_A and Sand_B)

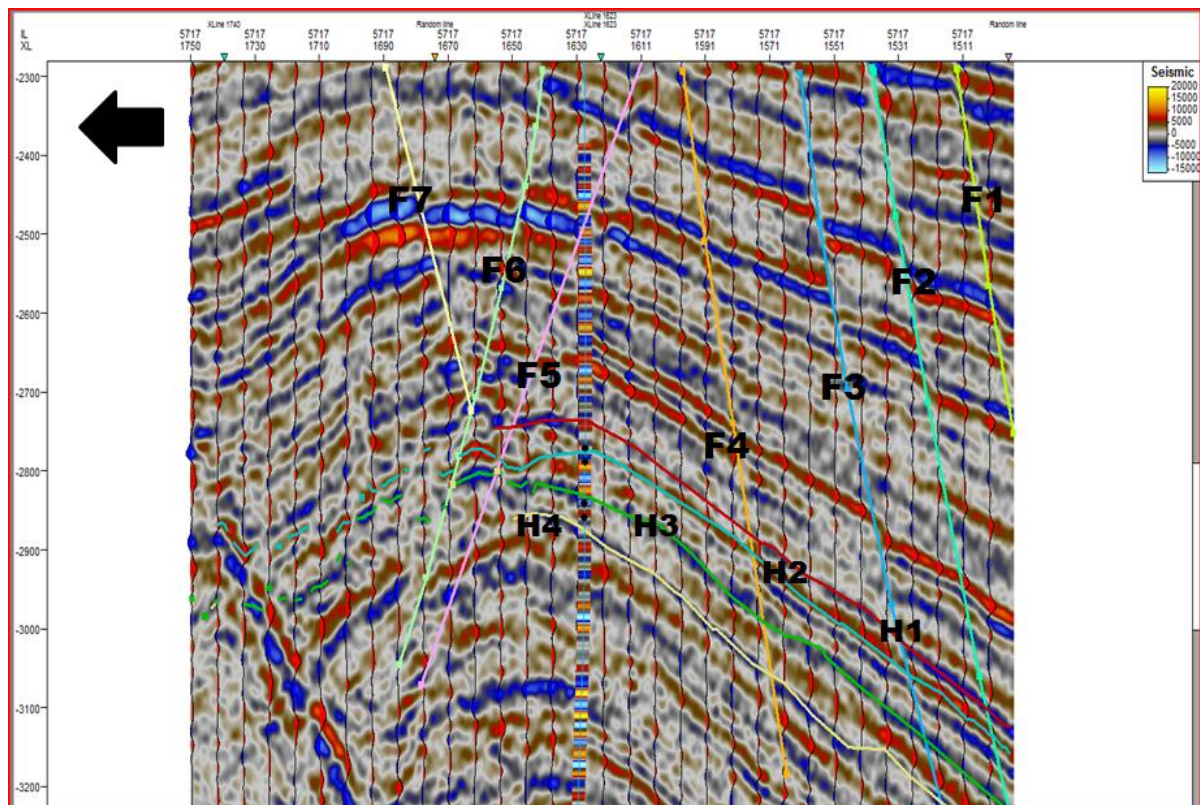


FIG 4.2 The vertical section (inline 5717) through well 2, showing the fault pattern and horizons (H1, H2, H3 and H4) picked

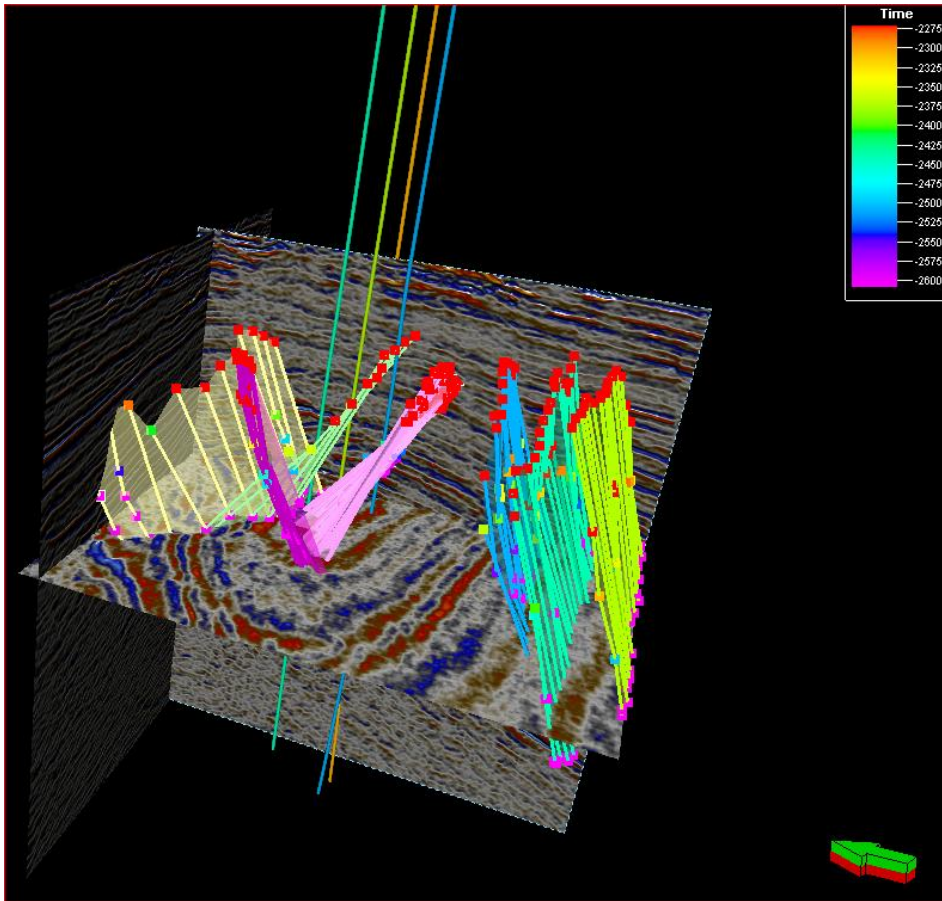


Fig 4.3; Seismic section of incline 5713 with time slice showing the fault geometry and the four wells

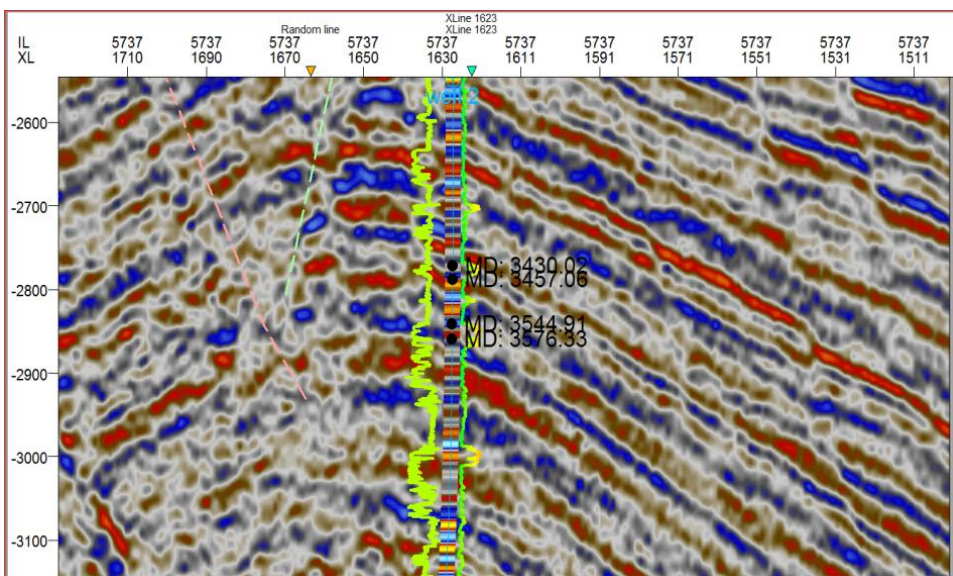


Fig 4.4; Well to seismic tie of the well tops (four black spots) conforming with GR and Resistivity log of well 2 on seismic section.

4.2.1 3-D SEISMIC TIME STRUCTURAL MAPS

4.2.2 Time structural map of horizons

Figures 4.5, 4.6, 4.7 and 4.8 shows the time structure map produced from the 3D Structural interpretation of the area of interest. The structural style of the four surface map are similar as a result of the closeness within horizons, structural highs are located at the north-eastern and spreads to the south west part of the field while the structural lows were observed in south east and north west region. The contour values on the structure map range from 2700 ms to 3300 ms. There are seven faults on the map and prominent faults (F6&F5) assisted closure exist at the North Eastern part of the map and dipping towards the western part. This type of contour configuration is indicative of an anticlinal structure that is favourable to hydrocarbon accumulation.

4.3 SEISMIC DEPTH STRUCTURAL MAPS

4.3.1 Depth structure map of Horizons.

Figure 4.9, 4.10, 4.11 and 4.12 depict the depth structural maps from the time to depth conversion using the checkshot of the field. The contour values range from 3300 m to 4250 m and the structural geometry of the surfaces are similar due to the closeness of the surfaces at the target interval. There is a variation in depth within the study location which thickens from the south-west to the north-east direction and is due to the structural deformation that has occurred in the area. The depth maps have seven faults with F6 and F5 faults having potential of fault dependent closure both at the north east and central part of the study area. The maps shows four wells were drilled around the study area for hydrocarbon exploitation at the flank of the anticlinal structure (Structural high) primarily because of its ability to accumulate hydrocarbon. The possible petroleum trapping system is the large roll over anticline located at the northeast and north central parts of the field. This is an indication that the crest of the anticlinal structure is the footwall while the wells drilled at the flank is on the down thrown block of the growth faults(F6 and F5)

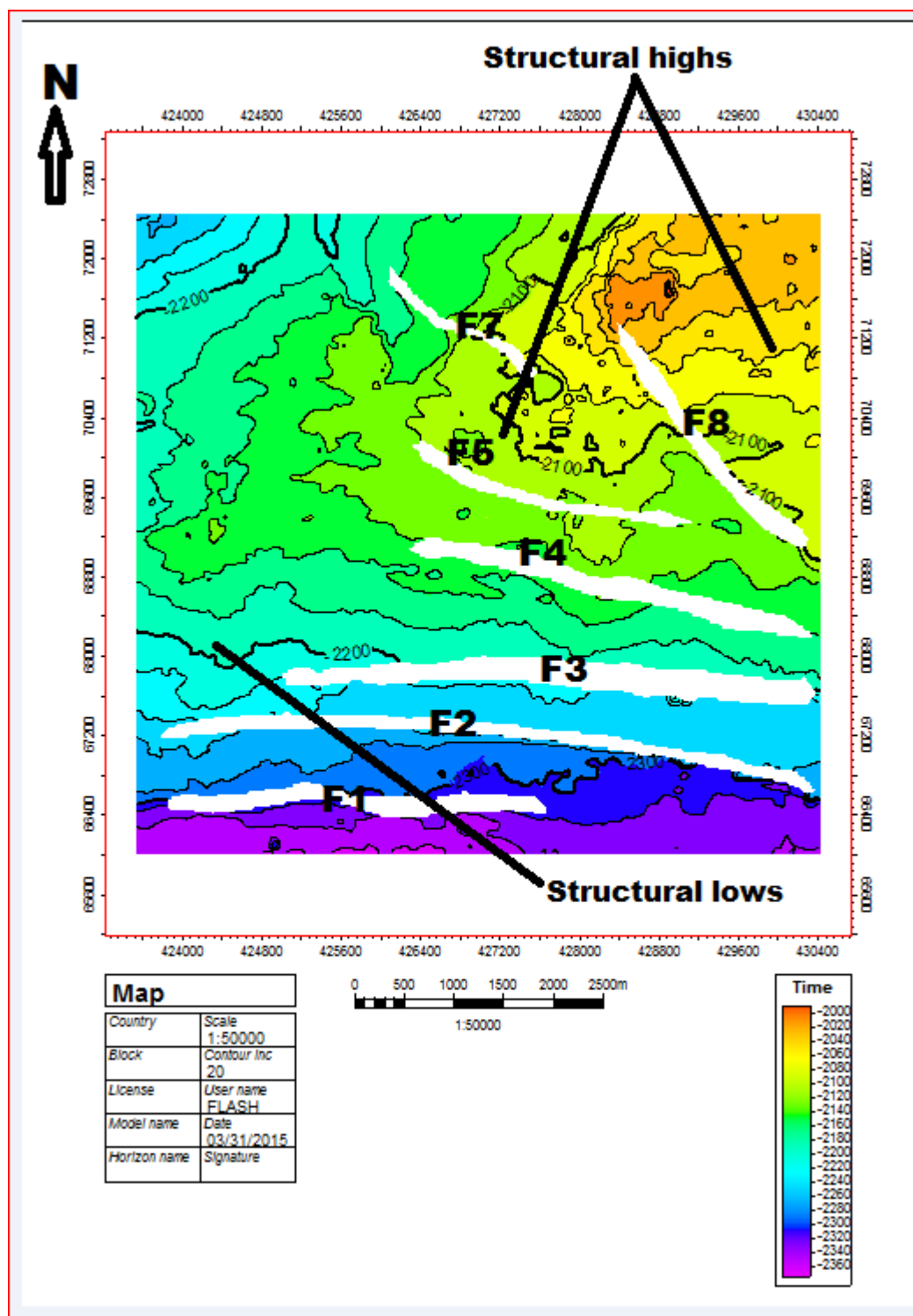


Fig 4.5 The event time structure map of horizon H1 (top surface of the Sand_A reservoir) at 2350ms showing the structurally high and low areas

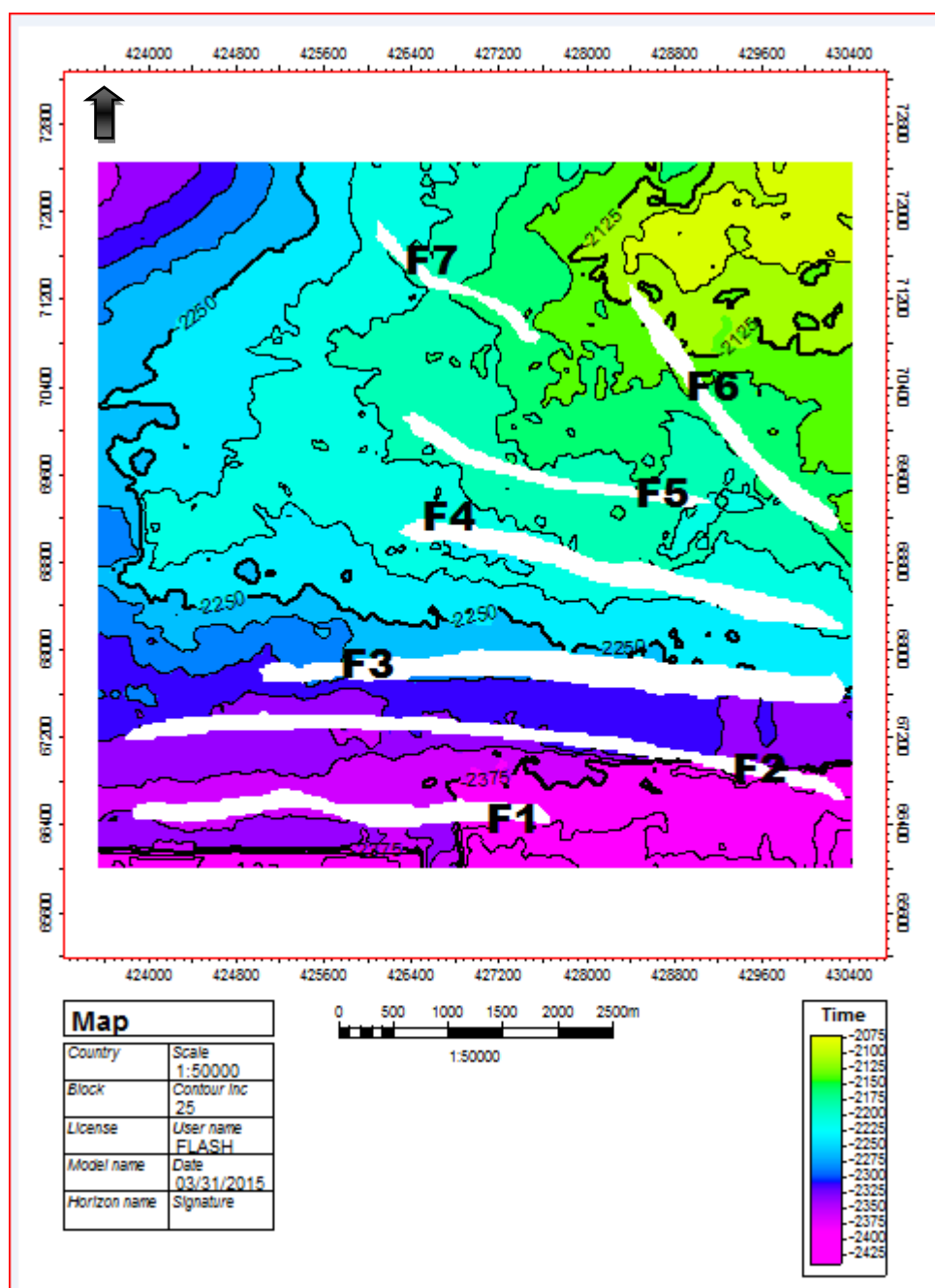


Fig 4.6 The event time structure map of horizon H2(base of Sand_A reservoir) at 2380ms

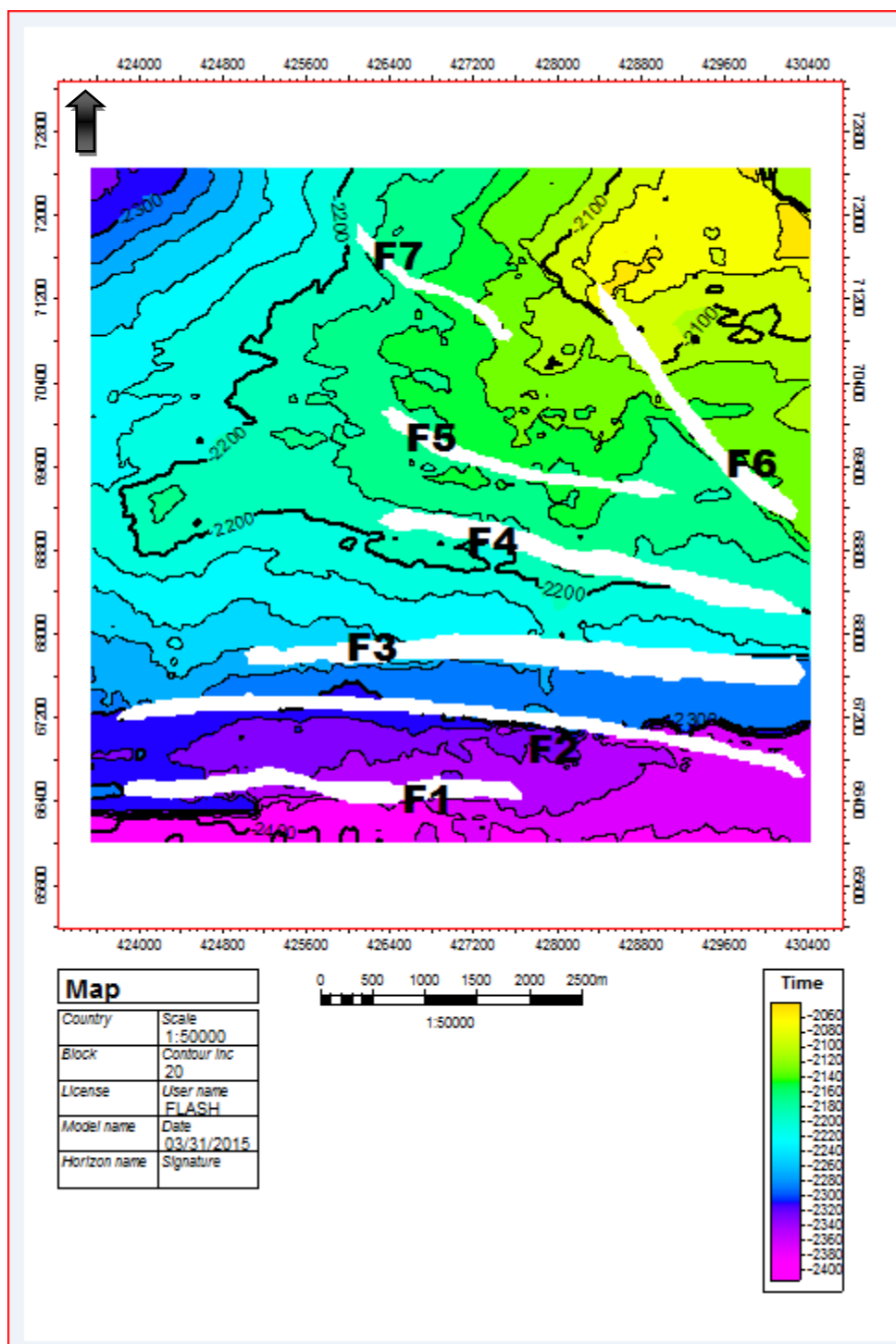


FIG 4.7 The event time structure map of horizon H3 (top of Sand_B reservoir) at 2400ms

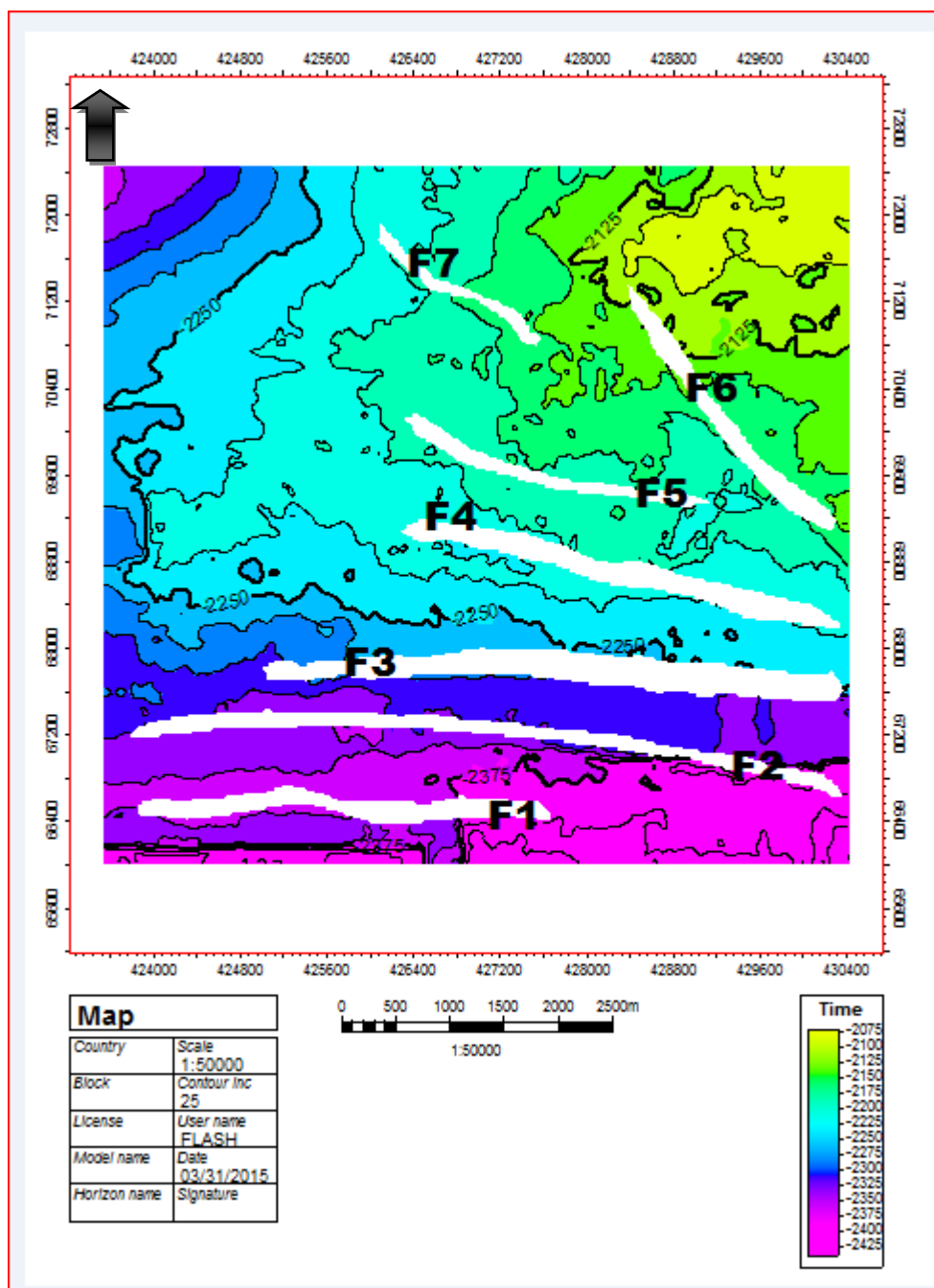


Fig 4.8 the event time structure map of horizon H4 (Base of Sand_B reservoir) at 2425ms

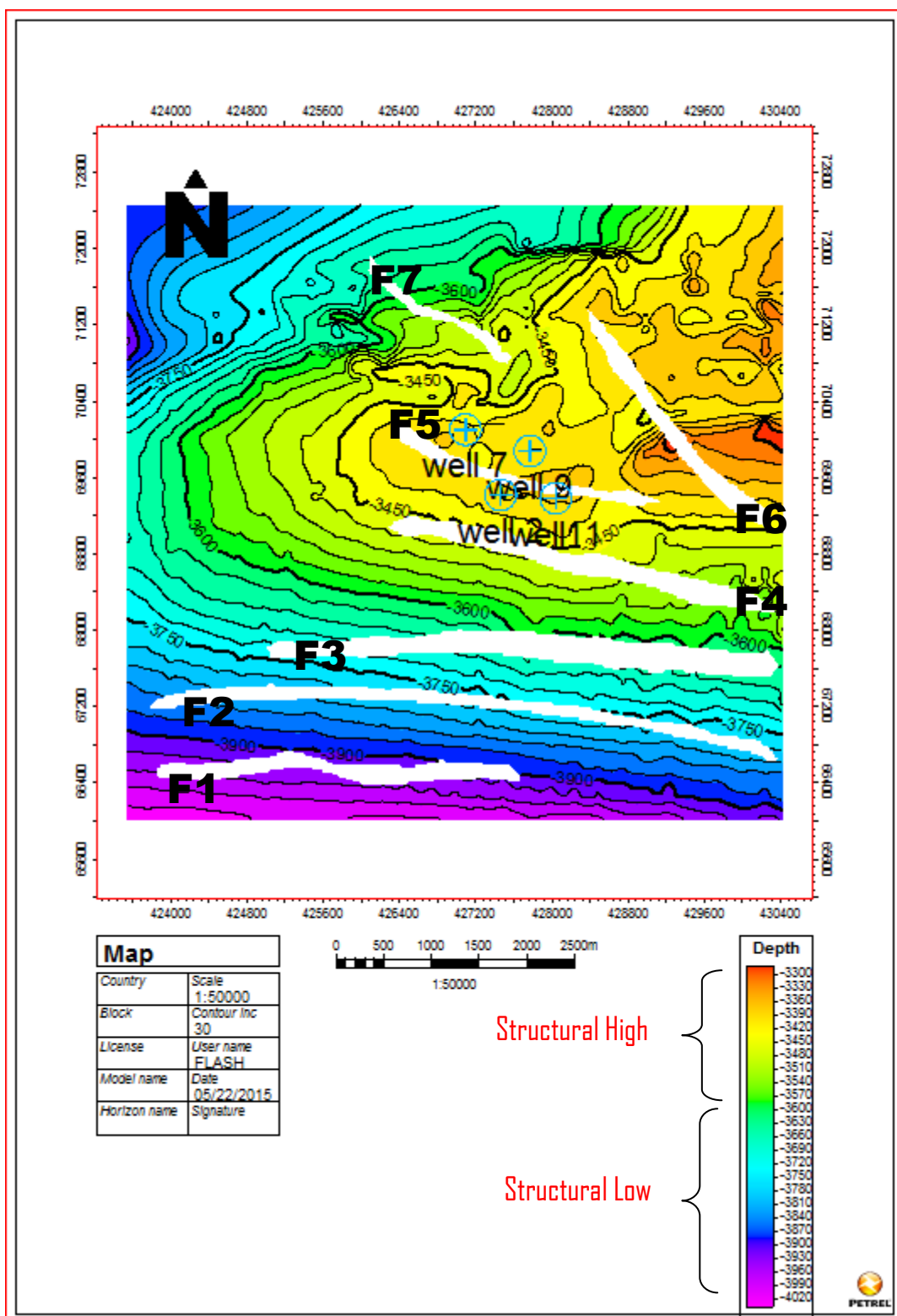


Fig.4.9: Depth structural map of the top of Sand_A Reservoir at 3300m

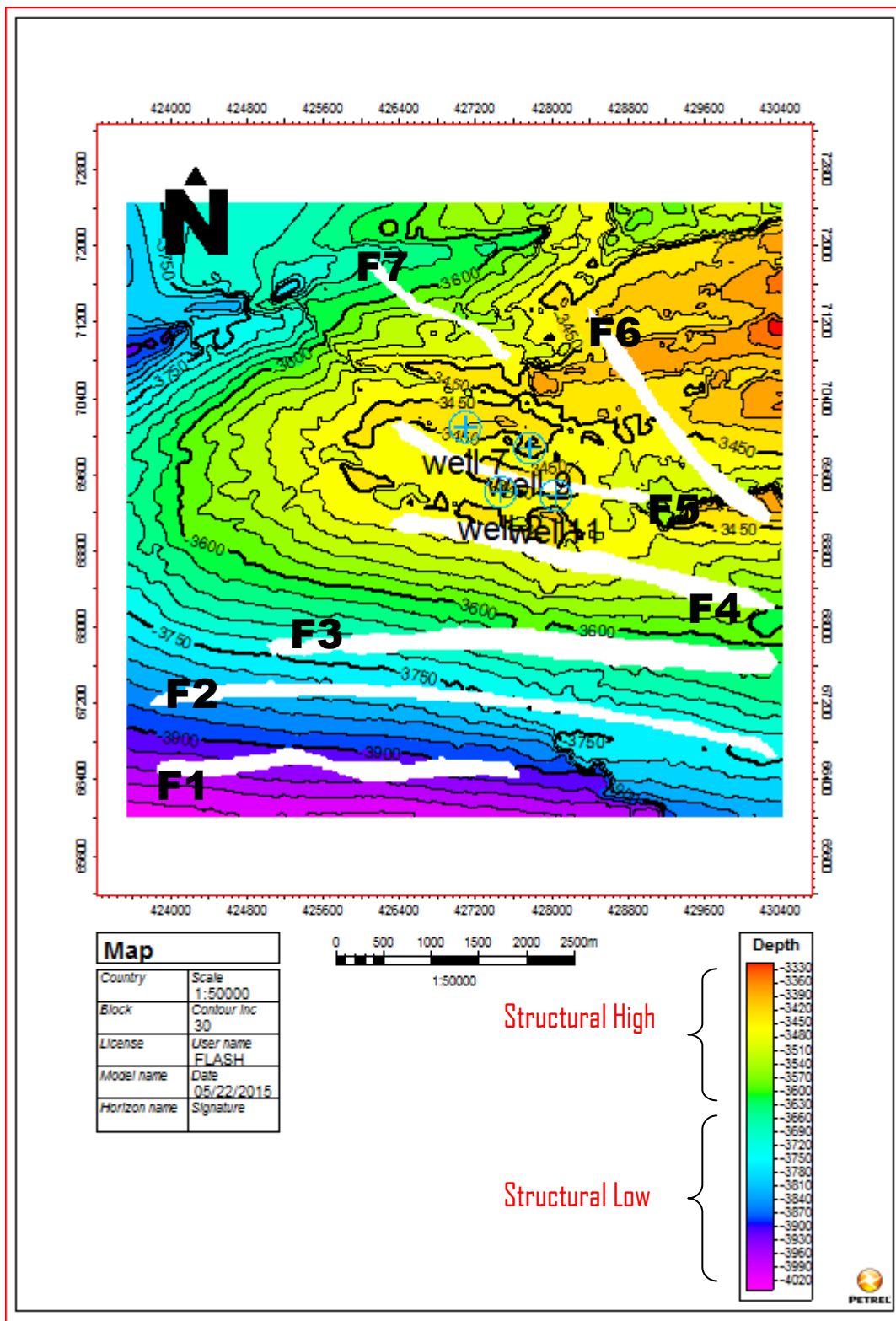


Fig 4.10; Depth structural map of the base of Sand_A Reservoir at 3400m

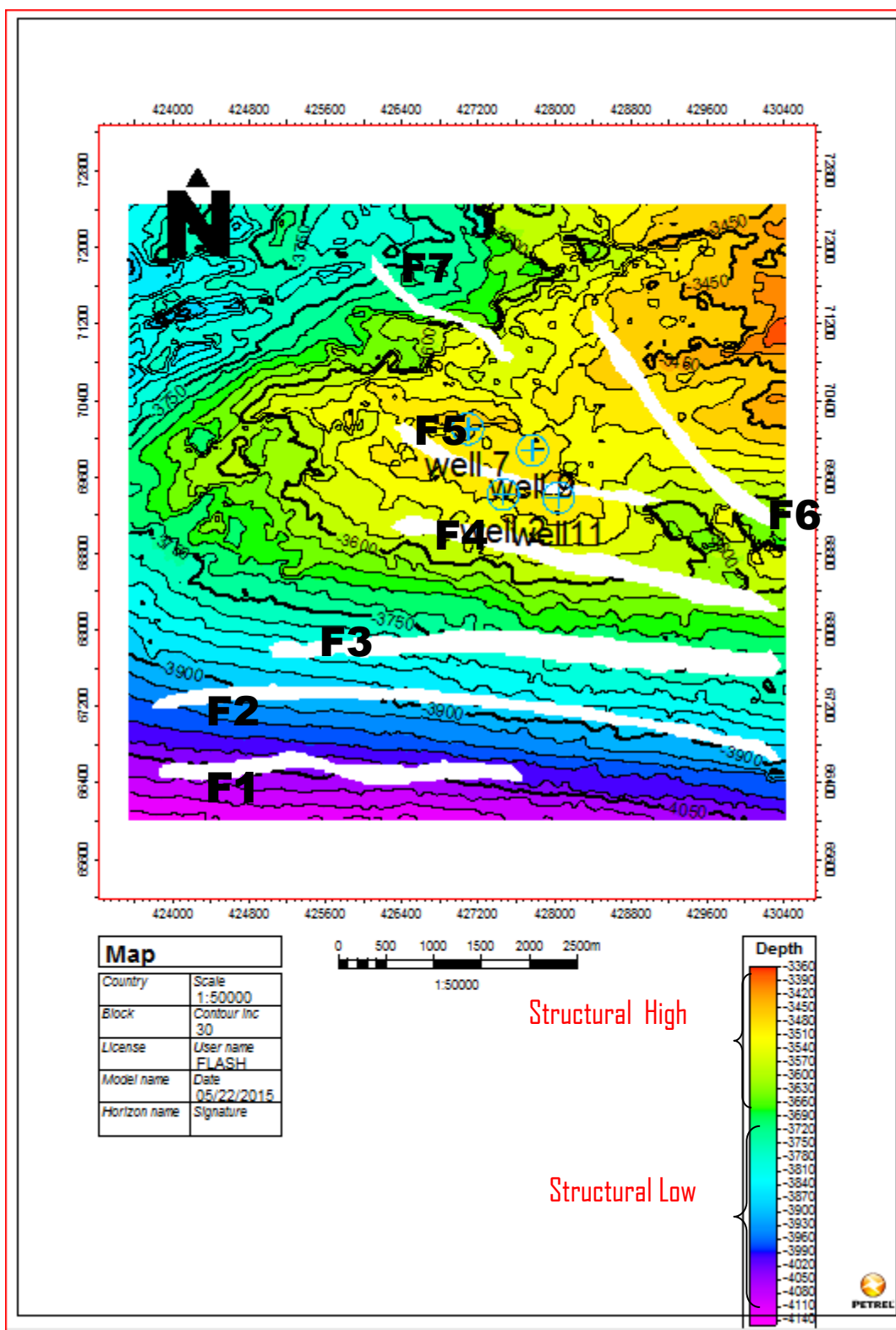


Fig 4.11; Depth structure map of the top of Sand_B Reservoir at 3450m

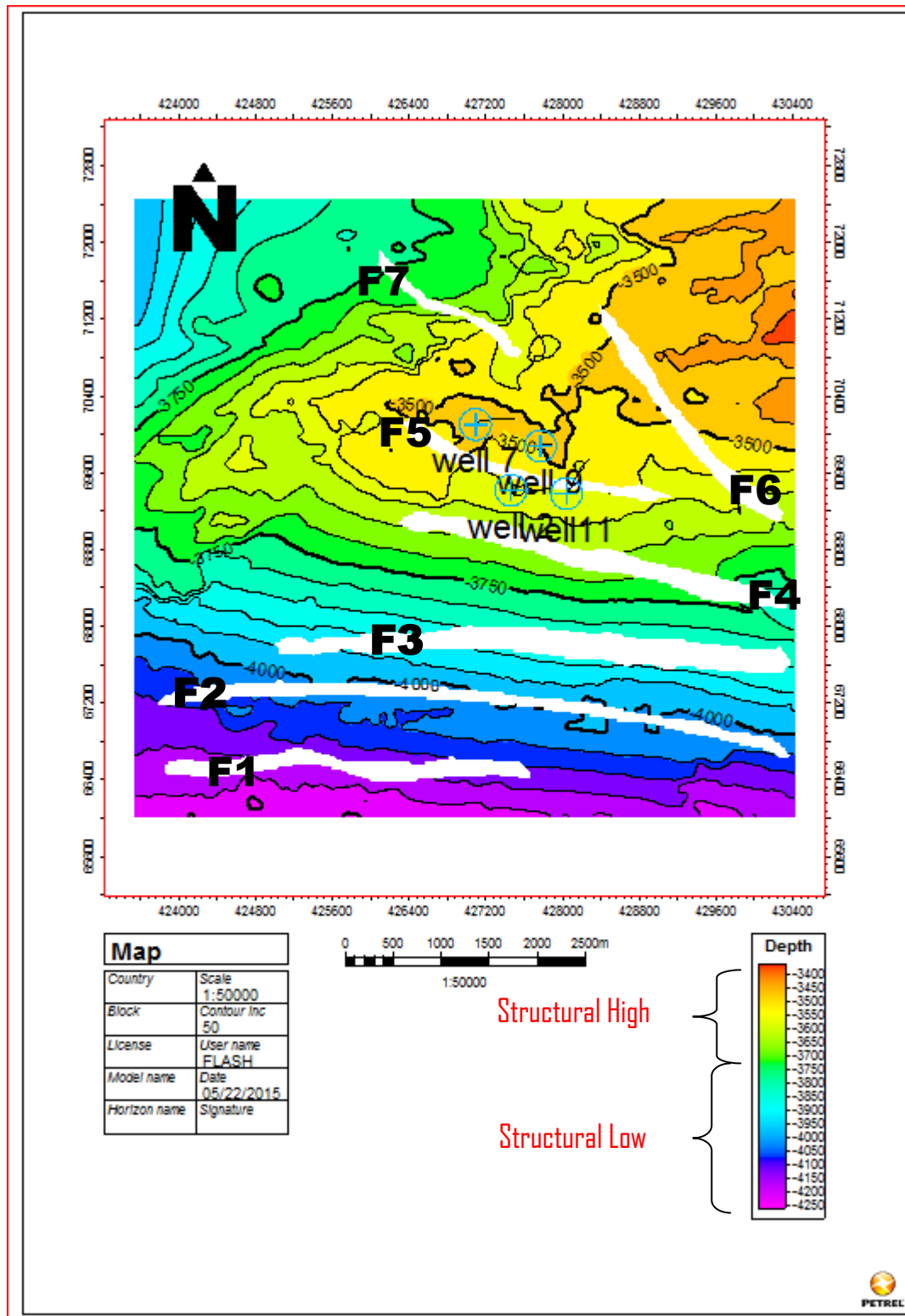


Fig.4.12: Depth structure map of the base of Sand_B Reservoir at 3500m

4.4 SEISMIC TIME SURFACE ATTRIBUTES

The idea of using amplitude extraction for analysis is from the assumption that lithology, rock properties and fluid content should affect seismic character also, for better analysis comparison is made with other textural attributes which defines sandstone distribution and connectivity of the hydrocarbon bearing facies of the reservoirs. Three surface attributes maps were generated for each of the four surfaces, Sand_A (top and base) and Sand_B (top and base). These are RMS amplitude, instantaneous frequency map and interval average extraction maps. These were carried out in order to delineate new reservoirs that may be hidden through structural traps and the lateral extent of the reservoir sand units. The seismic attribute extraction maps for horizon H1, H2, H3, H4 and the four wells well 2, well 7, well 9 and well 11 were shown in Figures 4.13-4.15.

4.4.1 EXTRACTION MAP INTERPRETATION

Fig 4.13 The RMS amplitude map of the various horizons show high amplitude zones limited to three major colours (sky blue, green, yellow). At the north east, south west and pockets around the south east area (prominent in H1 and H2), the high amplitude zones (sky blue) is believed to be hydrocarbon saturated sand units overlying shale (purple) due to acoustic impedance contrast. The sky blue and green coloured areas are seen as highly porous formation with hydrocarbon prospect, while the yellow zones is assumed to also be porous unit but with different fluid content and the background purple colour is proposed as a lateral change in lithofacies to non-porous formation. Bright spots tend to increase from the north east to the south west and south east (especially in H1 and H2). This indicates direction (NE-SW) of displacement of porous units hence depositional environment can be inferred to be point bar of distributary channels.

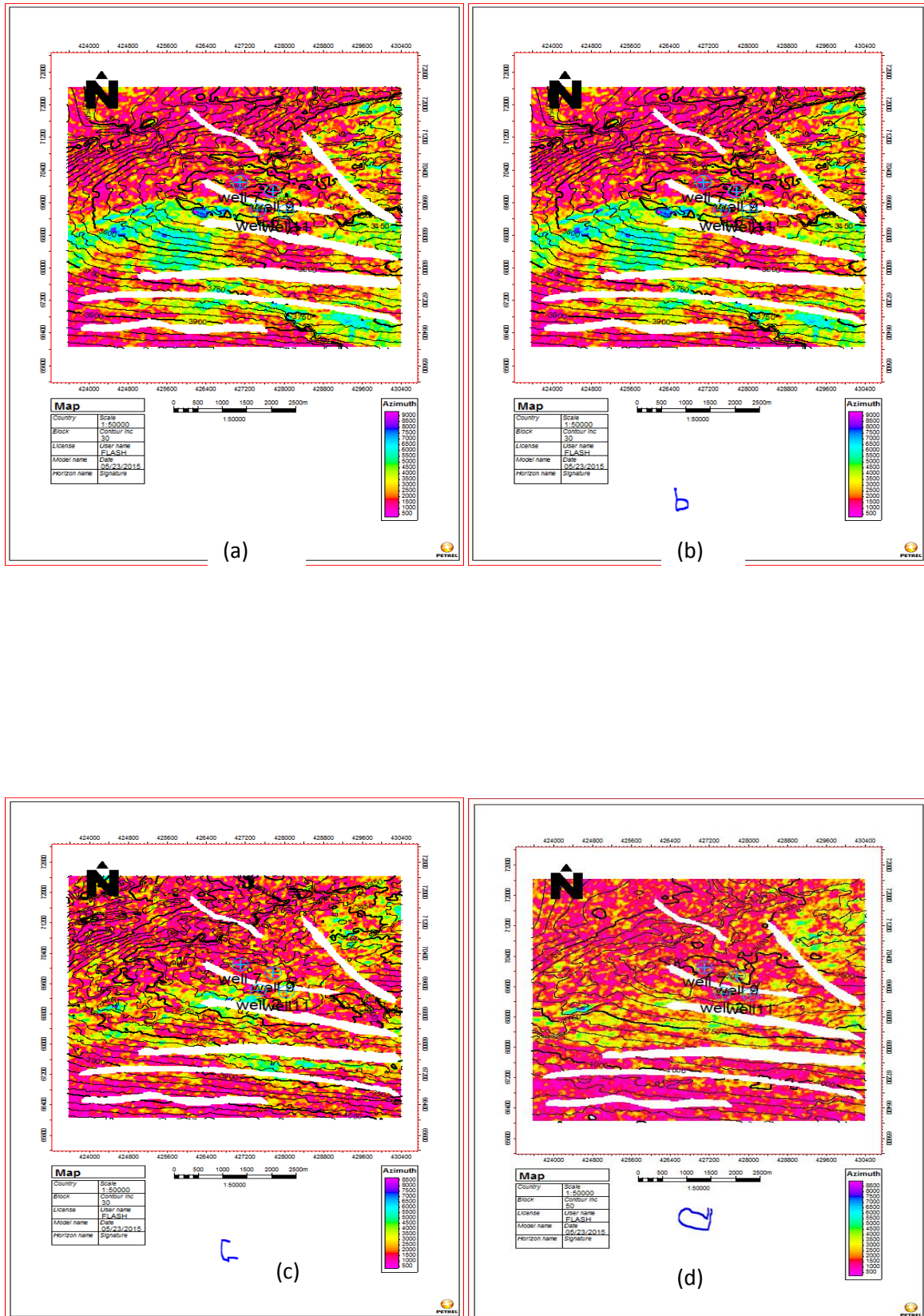
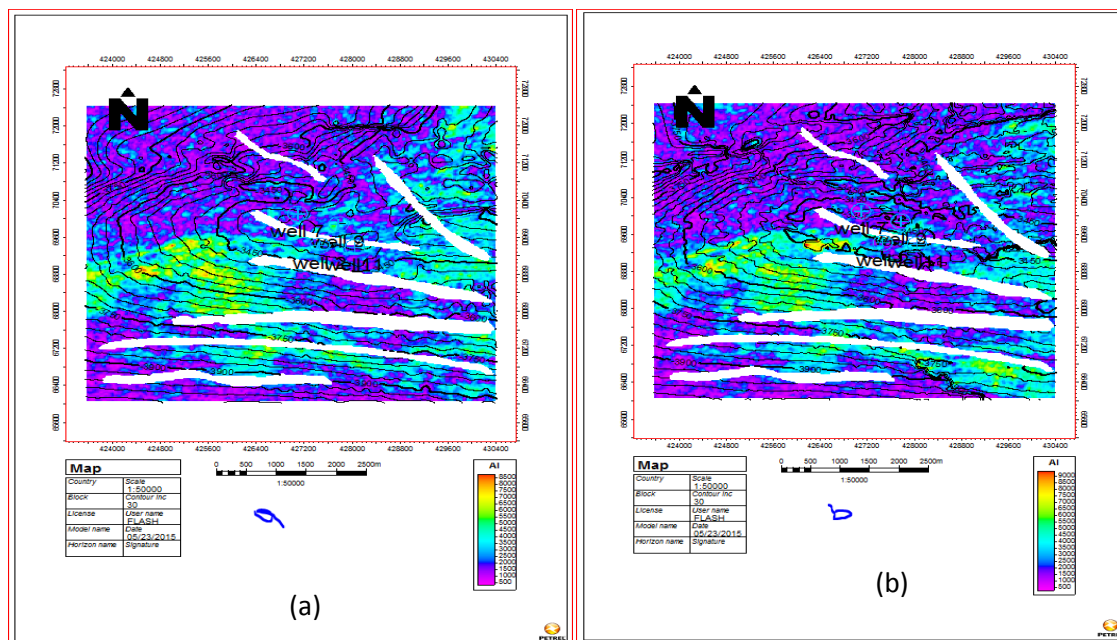


Fig 4.13; RMS Amplitude maps of the horizons (a) Horizon(H1) at 2750ms (b) Horizon (H2) at 2780ms (c) Horizon (H3) at 2800ms (d) Horizon (H4) at -2780ms showing high amplitude zones(sky blue) which is possible Hydrocarbon Accumulation(bright spots) areas.

Fig 4.14 Interval average extraction maps of the horizons shows similarity in lateral distribution, litho logic variation and hydrocarbon prospect zones. Bright spots which are a direct hydrocarbon indicator (DHI) were seen as a result of decrease in impedance of the sand unit and the intercalated shale. The bright spots (red and yellow) observed at the north east trending to the south west and south east zones on the surfaces (prominent on H1 and H2) explains that the south west zone is a younger sand unit(channel sand fills) as carrier beds conveying possible hydrocarbon into the respective traps basin ward. The high amplitude areas are seen on and around the structural high zone (NE-SW) which confirms why the wells are drilled at the anticlinal structure

Fig 4.14;Interval average extraction maps of the horizons (a) Horizon(H1) at 2750ms (b) Horizon (H2) at 2780ms (c) Horizon (H3) at 2800ms (d) Horizon (H4) at -2780ms showing high amplitude zones(red and yellow) which is possible Hydrocarbon Accumulation(bright spots) areas.



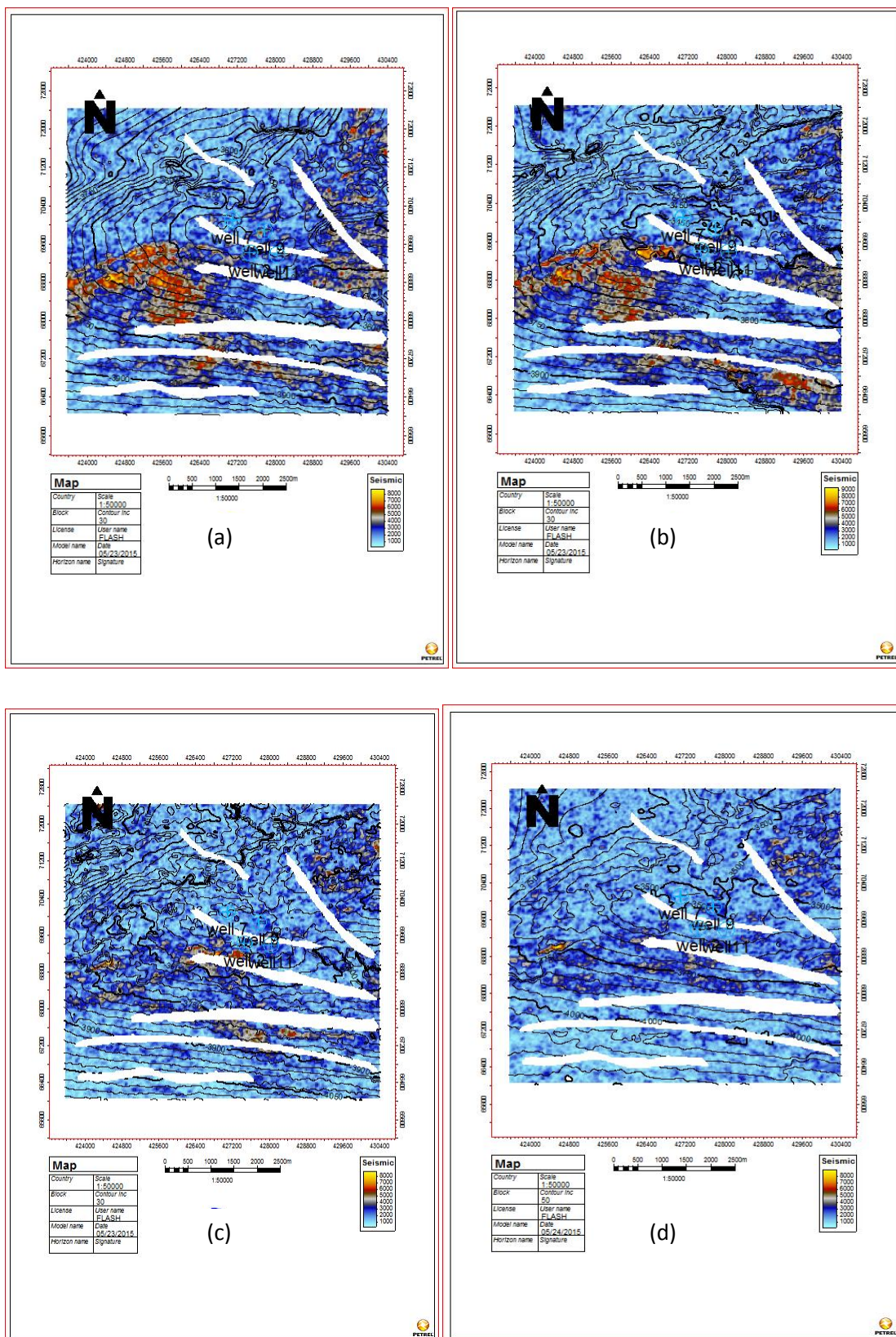


Fig 4.15

4.5 PETROPHYSICAL INTERPRETATION

The parameters deduced from the analysis include gamma ray index, porosity, net to gross, volume of shale, formation factor, irreducible water saturation, hydrocarbon saturation, water saturation and hydrocarbon pore volume. These parameters would help to effectively quantify the reservoirs in terms of the hydrocarbon pore volume and amount of hydrocarbon in place.

The petrophysical analysis began with the identification of reservoirs (sand bodies) within the Agbada Formation present in the well by observing intervals where the gamma ray reads relatively low values (i.e. deflects to the left). The fluid contact was determined using the resistivity log since hydrocarbon is more resistive than water. Based on the analysis, two hydrocarbon bearing zones A and B were identified for further interpretation. The petrophysical parameters are present in table 4.1& 4.2

Table 4.1: Showing the calculated petrophysical parameters for sand A (shallow reservoir)

	GROSS (m)	Vsh	Vsh (%)	Porosity (%)	F	Swirr (%)	K (Oil)	Sw	Sw (%)	N/G	N/G (%)	Shc (%)	HCPV
Well 7	33.86	0.49	49.0	19.1	25.7	11.1	309	0.35	35.0	0.22	22.4	64.6	12.0
Well 2	26.77	0.49	49.0	18.7	23.9	41.7	65	0.42	42.0	0.22	22.1	58.0	11.0
Well 9	26.32	0.49	49.0	18.7	24.4	10.97	63	0.32	32.0	0.22	22.2	67.7	12.0
Well 11	18.20	0.49	49.0	20.3	28.1	11.13	540	0.96	96.0	0.22	22.2	0.04	2.0

	Gross (m)	Vsh	Vsh (%)	Porosity (%)	F	Swirr (%)	K (oil)	Sw	Sw (%)	N/G	N/G (%)	Shc	Hcpv
Well 7	77.47	0.17	17	13.1	50.6	15.8	18	0.68	68	0.05	5.34	32	4.0
Well 2	49.13	0.82	82	14.9	40.7	37.7	80	0.38	38	0.12	12	62	9.0
Well 9	31.48	0.29	29	13.1	51.9	15.8	15	0.46	46	0.01	10	54	7.0
Well 11	53.59	0.17	17	13.1	15.6	15.8	18	0.69	69	0.05	5.34	31	4.0

Table 2: Showing the calculated petrophysical parameters for the sand_B

4.5.1 PETROPHYSICAL INTERPRETATION OF THE RESERVOIRS

From Tables 4.1 and 4.2, The petrophysical analysis have the porosity values of the reservoir Sand_A ranging from 18.1-20.3% and reservoir Sand_B ranging from 13.1-14.9% across the reservoir. The permeability values of reservoir Sand_A ranging from 63-540md and reservoir Sand_B ranging from 18-80md hence there is decrease in porosity and permeability of the field with depth. The Sw values for the reservoir ranges from 38-42% in well 2, 35.39-68.79% in well 7, 32.28-45.57% in well 9 and 68.79-96.06% in well 11. The volume of shale range from 17-82% across the Sand_B and 49% in reservoir Sand_A.

The petrophysical results of the wells (Table1) show fair porosity despite high Vsh (shaliness) cut offs ,porosity and permeability decreases from Sand_A at 3423m(shallow reservoir) to Sand_B at 3537m (deeper reservoir),the decrease in porosity and permeability with depth is due to compaction resulting from over burden.

The resistivity, porosity and density logs revealed that the reservoir are more of gas bearing zones, which verify the increase in gas to oil ratio seaward as a result of the high shale percentage in the coastal swamp depobelt (Doust ,1989)The Bulk Volume Water of the sand units is not constant across the wells indicating variation in water saturation and irreducible water($Sw > S_{irr}$) , geologically this showing that the reservoir may not produce water free hydrocarbon The reservoirs show roughly cylindrical log motif suggesting distributary channel depositional environment.

The reserve estimation confirms the reservoirs to be a marginal field and not economical, as the average hydrocarbon saturation across the reservoirs (<50%) has net pay that is more of gas than oil, high Vsh, poor porosity and permeability.

4.6 RESERVE ESTIMATION

Deterministic estimation of the volume of hydrocarbon in place (OOIP) involves the application of one or more simple equation that describes the volume of hydrocarbon filled pore space in the reservoir and the way the volume will change from the reservoir to the surface. These simple volumetric equations are used to derive petrophysical parameters, which includes: volume of shale, formation factor, porosity, water saturation, permeability, Gross Rock Volume, Net to Gross, irreducible water saturation, Hydrocarbon pore volume etc, hence, integrating the result from seismic interpretation to Estimate the Reserve of the Reservoir.

$$\text{OOIP} = \text{Volume of Oil Resources} * \text{Area covered by oil} \quad 4.1$$

This volume was calculated directly from the volume of oil resources contour map. The area of the map occupied by oil is calculated in sections with respect to the contour intervals. The individual area is then multiplied by the individual contour value to get the individual volumes. Finally, all the individual volumes are added to get the total volume of oil resources in the field which is equivalent to the volume of oil in place (OOIP). The unit here is stock tank barrels.

The hydrocarbon originally in place (OOIP) could also be computed directly using the average value for the net pay thicknesses, average hydrocarbon saturations and average porosity values and substituted in the following equations:

$$\text{OOIP} = (7758 * A_{\text{oil}} * h_{\text{oil}} * S_{\text{h(oil)}} * \phi_{\text{N-D}}) / b_o$$

A_{oil} = Area occupied by oil

h_{oil} = Average height of oil column

$S_{\text{h(oil)}}$ = Hydrocarbon saturation (oil column)

B_o = Formation oil volume factor = 1.2 bbls/STB

Table 4.3; Showing oil originally in place (OOIP) in the various wells
(RESERVE ESTIMATION)

WELLS	2	7	9	11
OOIP(mmbbls)	9.3	5.7	3.5	2.3

4.7 DISCUSSION

Based on the Information extracted from a three pronged approach, the 3-D seismic data volume and the suits of well logs with the integration of seismic attributes analysis have revealed that the structural geometry and stratigraphic style of the field agrees with the Agbada Formation of the Niger Delta, which is elaborated below;

The lithologic units (fig 4.1) are relatively consistent across the wells and predominantly sand, sandstone and shale with increasing trend of shale thickness and high sand/shale ratio indicates the Agbada formation, Niger Delta. Basically, the intercalations are the result of differential subsidence variation in the sediment supply and shifts of the delta depositional axes, which cause local transgressions and regressions as proposed by Short and Stumble (1965).

The northeast-southwest trending anticline, with associated fold related synthetic(F1,F2,F3,F4, &F7) and antithetic (F5 & F6) faults, interpreted to have been folded and faulted by localized compression resulting from a possible combination of differential loading in the deep-seated over pressured ductile under compacted marine Akata Shale gravitational collapse of slope and extensional and translational movement as infer by Doust and Omatsola (1989).

According to Abe and Olowkere (2013), they interpreted 3D seismic data set from continental slope, offshore Niger Delta integrating structural interpretation with seismic attributes, revealed high amplitude zone at the crest of the structural high zone which conforms with the possible hydrocarbon prospect zone (Bright spots) of the generated time surface attribute maps (Fig 4.12;4.13;4.14).

The petrophysical results of the wells (table 4.1 and 4.2) reveal fair porosity despite high volume of shale (shaliness) cut offs, porosity and permeability decreases with depth as a result of increase in over burden pressure resulting from compaction. Hence Sand _A (shallow reservoir) has better porosity and permeability than sand _B (deeper reservoir).

The resistivity, neutron porosity, compensated density logs of the wells revealed that the reservoirs are more gas bearing zones, which verifies the increase in gas to oil ratio

basinward as a result of high shale percentage in the coastal swamp and off shore depobelt (Doust and Omotsola 1990).

From the table 4.1 and 4.2, the bulk volume water of the sand _A and sand _B are not constant across the wells indicating variation in water saturation (S_w) and connate (Irreducible) water ($S_w > S_{irr}$). The relatively high water saturation supports the fact that shale volume is high (very fine grain), geologically this account for the reduced permeability of the reservoirs therefore reservoirs may not produce water free hydrocarbon. Also, from the GR logs of the well, the reservoirs show roughly cylindrical log motif suggesting distributary channel depositional environment of the Agbada formation by Weber and Daukoru (1975). The reserve estimation confirms that the reservoir is a marginal field, as the average hydrocarbon saturation across the reservoir (<50%) has net pay more of gas than oil.

CHAPTER FIVE: SUMMARY, CONCLUSION AND RECOMMENDATION

5.0 SUMMARY

The densely faulted Gurumara field shows typical geologic structural features of the Agbada Formation Niger Delta, which was evaluated and analysed by a three pronged approach; Petrophysical analysis, structural interpretation and 3D seismic attributes analysis.

The integration of this approach with 3-D seismic data, check shot data and a suite of well logs for four wells were analyzed using Petrel (seismic to simulation software). The objectives were to carry out a detailed formation evaluation, reservoir characterisation and a 3-D assisted structural interpretation of the densely faulted oil field in the coastal swamp depo-belt of the Niger Delta. RMS amplitude, instantaneous frequency map and interval average extraction maps were extracted on the horizons, which revealed the bright spots and Dim spots on it. The attributes were used to establish the diagnostic ability of 3D seismic attribute analysis in enhancing seismic interpretation, and the importance of petrophysical analysis in economic decision in E&P companies as well as researchers of the mid Miocene to Pliocene Agbada Formation reservoirs in the coastal swamp depobelt of the Niger Delta basin. The method adopted involved a delineation of the various lithologies from the gamma ray log, identification of reservoirs from the resistivity log, well correlation, determination of petrophysical parameters, horizon and fault mapping, time to depth conversion, attribute analysis and reserve estimation. Two reservoirs named Sand_A and Sand_B were mapped. The petrophysical analysis gave porosity values of reservoir Sand_A ranging from 18.1-20.3% and reservoir Sand_B ranging from 13.10-14.9% across the reservoir. The permeability values of reservoir Sand_A ranged from 63-540md while for reservoir Sand_B it ranged from 18-80md. The Sw values for the reservoir ranges from 38-42% in Well 2, 35.39-68.79% in well 7, 32.28-45.57% in well 9 and 68.79-96.06% in well 11. The volume of shale range from 17-82% across the reservoir Sand_B and 49% in reservoir Sand_A. Seven faults labelled F1, F2, F3, F4, F5, F6, and F7 and Four horizons were mapped. Depth structure maps generated showed a massive Northeast-Southwest trending anticlinal structure. The Reserve estimation was calculated using the empirical formula method with the petrophysical parameter, hence well 2 has 9.3 mmbbls, well 7 has 5.7mmbbls, well 9 has

3.5mmbls and well 11 has 2.3mmbls. The petrophysical analysis revealed the presence of oil with a volume that is however not favourable for commercial exploitation. These techniques proved to be very reliable and useful in reservoir characterization and formation evaluation.

5.1 CONCLUSION

The formation evaluation and reservoir characterisation of Guramala field revealed the two major lithological units in the area to be sand and shale. In some parts of the Niger Delta opportunities have been captured at the shallow, intermediate and deep levels (Olowokere, 2009b). An anticlinal structure was observed on the depth map in the Northeast and stretching to the southwest of the study area, dipping towards the southwest. Seven faults labelled F1, F2, F3, F3, F4, F5, F6 and, F7 were continuous across the field.

The structural disposition of the four horizons mapped greatly favours the accumulation of hydrocarbon but the poor to fair reservoir parameters obtained from the wells indicate economic viability is slim. The interval average, RMS and instantaneous extraction maps from the horizons revealed high amplitude and bright spot areas around the structural highs which coincided with locations where producing wells well 2, well 7, well 9 and well 11 had already been drilled thereby validating earlier interpretations that led to their drilling. Two reservoir named Sand_A and Sand_B was mapped. The petrophysical analysis gave the porosity values of the reservoir Sand_A ranging from 18.1-20.3% and reservoir Sand_B ranging from 13.1-14.9% across the reservoir. The permeability values of reservoir Sand_A ranging from 63-540md and reservoir Sand_B ranging from 18-80md hence there is decrease in porosity and permeability of the field with depth. The Sw values for the reservoir ranges from 38-42% in well 2, 35.39-68.79% in well 7, 32.28-45.57% in well 9 and 68.79-96.06% in well 11. The volume of shale range from 17-82% across the Sand_B and 49% in reservoir Sand_A. The result of original oil in place for all the wells calculated shows that well 2 has the highest value with 9.3mmbls. In conclusion, the result of the seismic interpretation and petrophysical analysis shows that the reservoirs under consideration have a poor to fair hydrocarbon (oil) prospect.

5.2 RECOMMENDATION

All distortion effect, whether near-surface or amplitude related (for seismic data); high frequency noise, well bore washout, casing points, mud filtrate invasion, gaps, missing data or insufficient log suites (for well data) are taken care of or totally eliminated during data application or processing. Secondly, an enhanced research work will require more wells drill

at the study area for better lateral resolution and analysis. Therefore based on observation in this study, we recommend the drilling of more wells for acquisition of more data eg core data, mud log, and other disparate data sources so as to aid in reducing uncertainties and optimise producibility of the “GURUMARA FIELD”.

REFERENCES

- Avbovbo, A. A., 1978. Tertiary lithostratigraphy of Niger Delta; American Association of Petroleum Geologists Bulletin, vol. 62, pp. 295-300.
- Beka, F. T., and Oti, M. N., 1995. The distal Offshore Niger Delta: frontier prospects of a mature petroleum province, *in*, Oti, M.N., and Postma, G., eds., *Geology of Deltas*: Rotterdam, A.A. Balkema, pp. 237-241.
- Brown, A., 1996. Seismic Attributes and classification; *The Leading Edge*, vol. 13, p. 1090
- Brown, A.R., 2000. "Interpretation of three-dimensional seismic data" *A.M. Assoc. pet. Geol. Memoir* 42.
- Burke, K., 1972. Longshore drift, submarine canyons, and submarine fans in development of Niger Delta: American Association of Petroleum Geologists, vol. 56, p. 1975-1983.
- Churlin, V.V., and Sergeyev, L.A., 1963. Application of Seismic Surveying to Recognition of production part of Gas-Oil Strata; *Geologiya Nefti i Gaza*, vol. 7, no. 11; p. 363.
- Doust, H., and Omatsola, E., 1990, Niger Delta, *in*, Edwards, J. D., and Santogrossi, P.A., eds., *Divergent/passive Margin Basins*, AAPG Memoir 48: Tulsa, American Association of Petroleum Geologists, p. 239-248.
- Ebrom, D., 2004. The low-frequency gas shadow on Seismic section; *The Leading Edge*, vol. 23, p. 772.
- Ejedawe, J.E., 1981, Patterns of incidence of oil reserves in Niger Delta Basin: American Association of Petroleum Geologists, v. 65, p. 1574-1585.
- Ekweozor, C. M., Okogun, J.I., Ekong, D.E.U., and Maxwell J.R., 1979, Preliminary organic geochemical studies of samples from the Niger Delta, Nigeria: Part 1, analysis of crude oils for triterpanes: *Chemical Geology*, v 27, p. 11-28.
- Evamy, B.D., Haremboure, J., Kamerling, P., Knaap, W.A., Molloy, F.A., and Rowlands, P.H., 1978, Hydrocarbon habitat of Tertiary Niger Delta: American Association of Petroleum Geologists Bulletin, v. 62, p. 277-298.
- Evamy, B.D., Haremboure, J., Kamerling, P., Knaap, W.A., Molloy, F.A., and Rowlands, P.H., 1978. Hydrocarbon habitat of Tertiary Niger Delta: American Association of Petroleum Geologists Bulletin, v. 62, p. 277-298.
- Frost, B.R., 1997. A Cretaceous Niger Delta Petroleum System, *in*, *Extended Abstracts, AAPG/ABGP Hedberg Research Symposium, Petroleum Systems of the South Atlantic Margin*, vol. 15.

Haack, R.C., Sundararaman, P., and Dahl, J., 1997, Niger Delta petroleum System, *in*, Extended Abstracts, AAPG/ABGP Hedberg Research Symposium, Petroleum Systems of the South Atlantic Margin, vol. 20.

Hospers, J., 1965. Gravity field and structure of the Niger Delta, Nigeria, West Africa: Geological Society of American Bulletin, v. 76, p. 407-422.

Kulke, H., 1995. Nigeria, *in*, Kulke, H., ed., Regional Petroleum Geology of the World. Part II: Africa, America, Australia and Antarctica: Berlin, Gebrüder Borntraeger, p. 143-172.

Nton M. E. and Adesina A. D. 2009. Aspects of structures and depositional environment of sand bodies within tomboy field, offshore western Niger Delta, Nigeria, Materials and Geoenvironment, 56(3), 284–303.

Nwachukwu, S.O., 1972. The tectonic evolution of the southern portion of the Benue Trough, Nigeria: Geology Magazine, v. 109, p. 411-419.

Nwajide, C.S., 2013. Geology of Nigeria's Sedimentary Basins. CSS Bookshops Limited, Lagos, Nigeria. ISBN: 978-978-8401-67-4.

Opara, A.I., 2010. Prospectivity Evaluation of "Usso" Field, Onshore Niger Delta Basin, Using 3-D Seismic and Well Log Data. Petroleum & Coal 52 (4) 307-315, 2010.

Opara, A.I., Anyim, U.O., and Nduka, V., 2011. "3D Seismic Interpretation and Structural Analysis of "Ossu" Oil Field, Northern Depobelt, Onshore Niger Delta, Nigeria". Pacific Journal of Science and Technology. 12(1): 502-509.

Shannon, P. M., and Naylor N., 1989, Petroleum Basin Studies: London, Graham and Trotman Limited, p 153-169.

Sheriff, R. E. and Geldart, L. P. (1995). Exploration Seismology (2nd ed.) Cambridge University Press. pp. 209–210. ISBN 0-521-46826-4.

Sheriff, Robert E. (1991). "Geophysics": Encyclopedic Dictionary of Exploration Geophysics (3rd Ed.). Society of Exploration. ISBN 978-1-56080-018-7.

Short, K. C., and Stäuble, A.J., 1965, Outline of geology of Niger Delta: American Association of Petroleum Geologists Bulletin, v. 51, p. 761-779.

Stacher, P., 1995, Present understanding of the Niger Delta hydrocarbon habitat, *in*, Oti, M.N., and Postma, G., eds., Geology of Deltas: Rotterdam, A.A. Balkema, p. 257-267.

Olowokere, M.T., Abe, S.J., 2013. Structure and Facies Development Resulting From Neogene Gravity Tectonics and Depositional Processes: Application to Afo Field Niger Delta, Nigeria

Orife, J., Avbovbo, A., 1982. Stratigraphic and unconformity traps in Niger Delta, The Deliberate search for the subtle trap; AAPG memoir, vol. 32, pp. 251-265

Tuttle, M.L.W., Charpentier, R.R. and Brownfield, M.E., 1999. The Niger Delta Basin Petroleum System: Niger Delta Province, Nigeria, Cameroon, and Equatorial Guinea, Africa; Open- File Report 99-50-H, United States Geological Survey
World Energy Report, 44pp.

Weber, K. J., and Daukoru, E.M., 1975, Petroleum geology of the Niger Delta: Proceedings of the Ninth World Petroleum Congress, volume 2, Geology: London, Applied Science Publishers, Ltd., p. 210-221.

Weber, K.J., 1987, Hydrocarbon distribution patterns in Nigerian growth fault structures controlled by structural style and stratigraphy: Journal of Petroleum Science and Engineering, v. 1, p. 91-104.

Whiteman, A., 1982, Nigeria: Its Petroleum Geology, Resources and Potential: London, Graham and Trotman, p.394 .

Yilmaz, Öz, (2001). Seismic data analysis: processing, inversion and interpretation of seismic data, vol 1. Society of Exploration Geophysicists.ISBN 1-56080-094-1.

Yilmaz, Oz, Doherty, S. M., (1987). Seismic Data Processing (investigations in Geophysics), vol 2.Society of Exploration Geophysics. ISBN: 978-0931830402.